

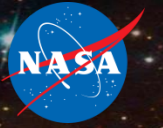


# Liquid hydrogen tank chill and no-vent fill prediction using computational fluid dynamics

**Justin M. Pesich, Daniel M. Hauser, Barbara A. Sakowski**  
*NASA Glenn Research Center*

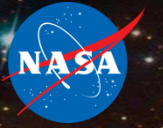
**Kiyotaka G. Yamashita, Michael C. Baker**  
*HX5, NASA Glenn Research Center*

Cryogenic Engineering Conference, 9-13 July 2023  
Honolulu, HI

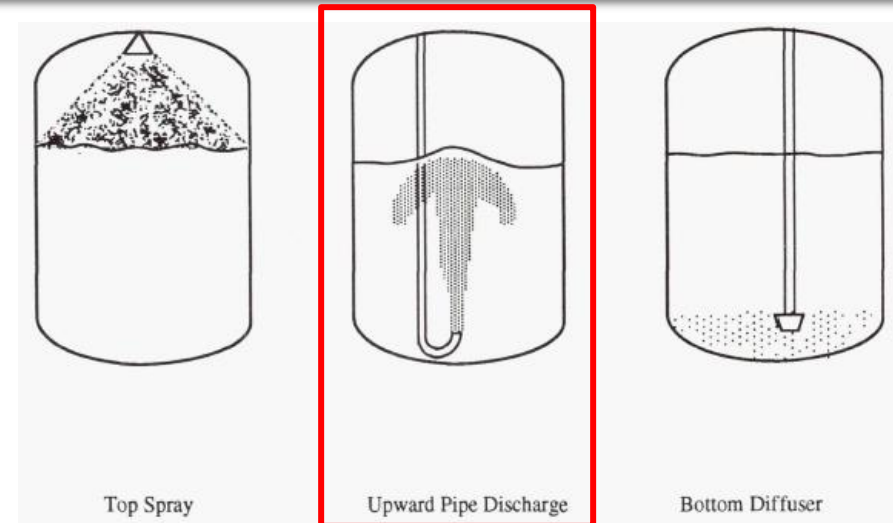


- On-orbit propellant depots for refueling spacecraft can support and enable NASA's long-duration deep space missions
- Cryogenic tank chill and fill is an important cryogenic fluid management (CFM) technology required to realize in-space propellant transfer
- No-Vent Fill (NVF) propellant transfer architectures require the receiver tank pressure to remain below the supply tank pressure during the entire transfer
- Accurate computational models can be used to reduce cost and risk, but these models must be validated to experimental data

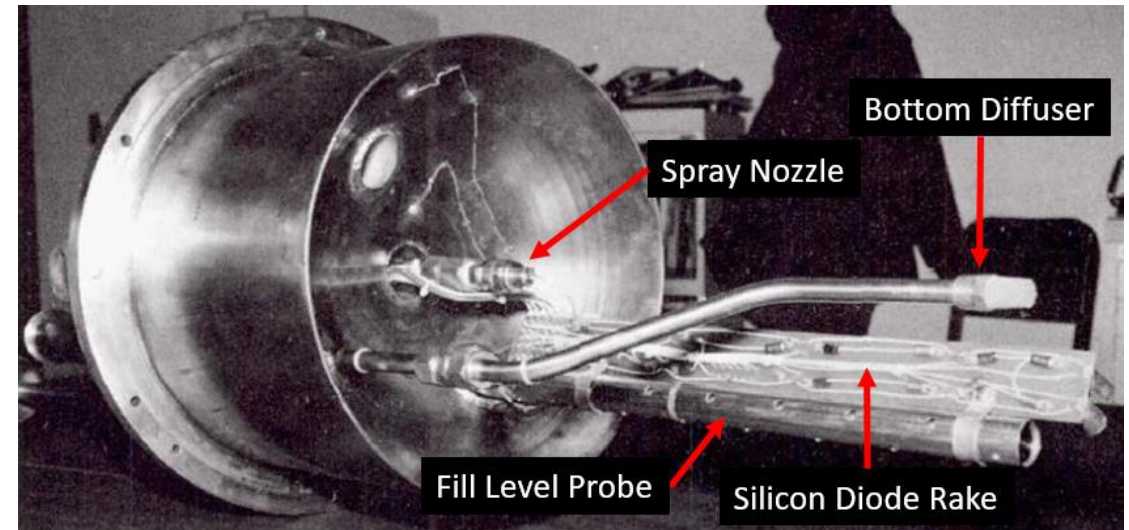
# Experimental Overview (1 of 2)



- Liquid Hydrogen NVF ground testing was conducted in 1990 at NASA Lewis Research Center (now Glenn Research Center)
- Cylindrical tank with elliptical domes
  - 20" height
  - 12.5" diameter
  - 1.2 cubic foot volume (34 liters)
- Experiment employed three different liquid injection methods: top spray, upward pipe, bottom diffuser
- Current work modeled the upward pipe discharge configuration



Liquid injection configurations used for NVF testing (NASA TM-105273, 1991)



Receiver tank lid assembly (NASA TM-105273, 1991)

# Experimental Overview (2 of 2)



- Experimental Measurements Taken:

- Tank Pressure
  - Fluid Temperatures
  - Solid Wall Temperatures
  - Fill Level
  - Mass Flow Rate
  - Inlet Temperature
- Reported as  $f(t)$
- Reported as  $\overline{f(t)}$

Measured Test Quantities for Test Number 9093G (NASA TM-105273, 1991)

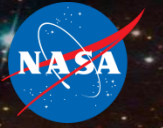
Fill Config	Inlet Venturi Temp	Inlet Venturi Flow Rate	Initial Tank Pressure	Final Fill Level
	K	kg/s	psia	% by volume
Upward Pipe	18.55	0.034	3.8	96

↳  $P_{\text{sat}}(T_{\text{inlet}}) \approx 8.2 \text{ psia}$

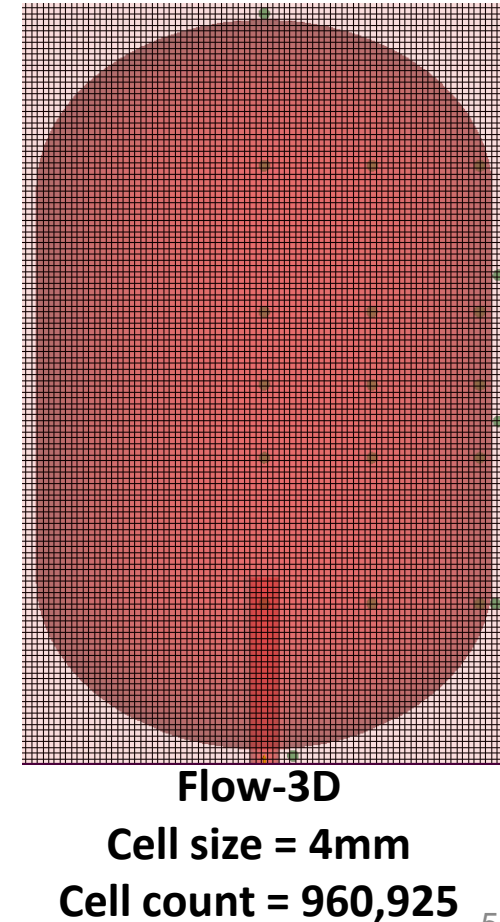
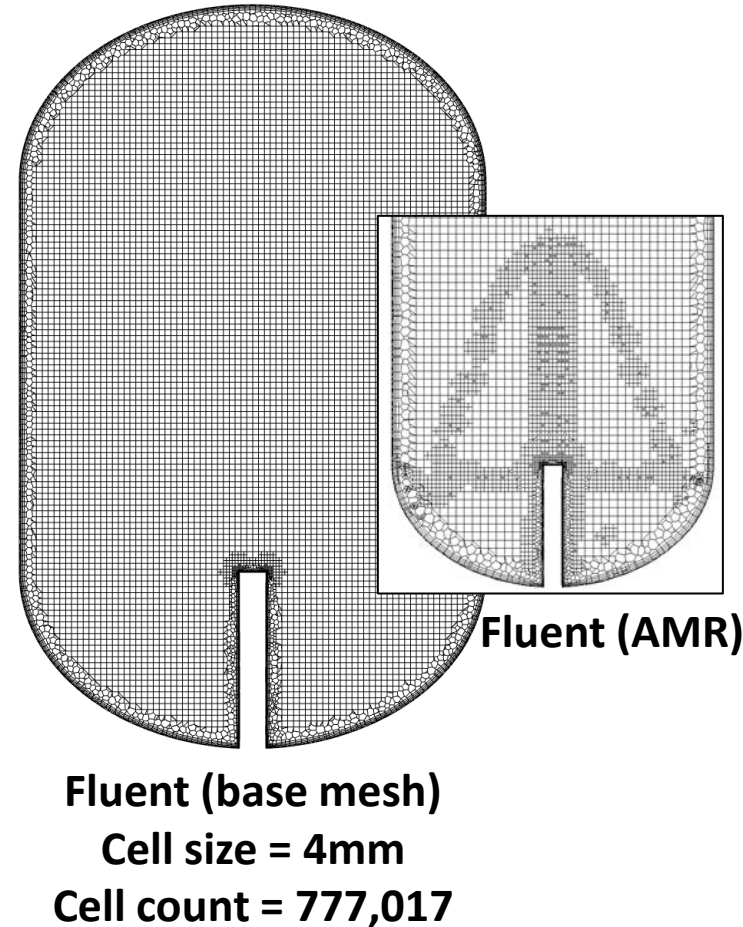
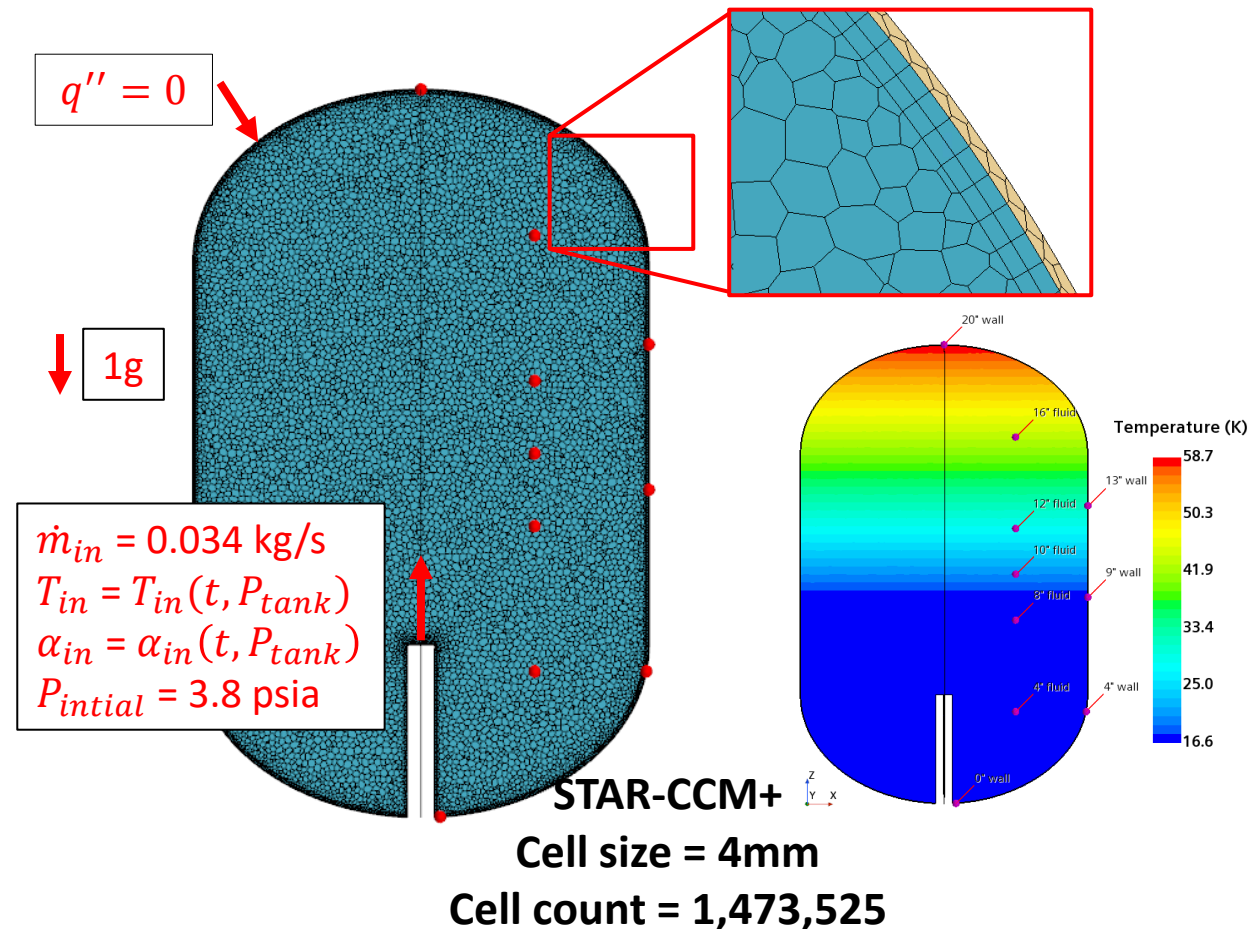
- Notable Sources of Experimental Uncertainty

- Geometric dimensions of injection pipe diameter, axial height of pipe exit, tank lid assembly, and tank wall thicknesses
- Mass flow rate and inlet temperature reported as averaged quantities (no time-dependent data)
- Heat leak
- **% of Helium in tank at start of test, if any (Helium gas was used to purge tank between tests)**

# Computational Model: Geometry/Mesh, and Boundary and Initial Conditions



- Three different commercial CFD codes were used to model the problem: STAR-CCM+ (J. Pesich), Fluent (K. Yamashita), Flow-3D (M. Baker)
- Full 3D geometry with the solid wall to model the conjugate heat transfer
- Initial temperature field set to match experimental wall temperatures using linear interpolation between probes





- Volume-of-Fluid Multiphase Solver
- Surface Tension Force with 0deg contact angle
- Constant liquid properties, compressible ideal gas
- Temperature-dependent SS304 properties ( $C_p$  and  $k$ )
- $Re_d = 1.4e5 \rightarrow$  turbulent flow
- Schrage Equation for user-defined interfacial mass transfer with Accommodation Coefficient,  $\sigma$
- Conservation of Enthalpy for liquid flashing across an orifice was used to calculate inlet quality and void fraction every time step
  - Initial tank pressure is well below saturation pressure at inlet temperature so liquid will flash as it enters tank
  - Inlet Void Fraction and Inlet Temperature function of time as it adjusts to current tank pressure predicted by CFD
  - Inlet Temperature flashes to  $T_{sat}(P_{tank})$  until  $P_{tank} \geq P_{sat}(T_{inlet,exp})$

## Schrage Equation for Interfacial Mass Transfer

$$\dot{m}_i = \left( \frac{2\sigma}{2 - \sigma} \right) \sqrt{\frac{M}{2\pi RT_{cell}}} (P_{sat}(T_{cell}) - P_{abs}) \left[ \frac{kg}{m^2s} \right]$$
$$\sigma = 0.001$$

## Clausius-Clapeyron Relation

$$P_{sat}(T_{cell}) = P_{ref} \exp \left[ \frac{L}{R} \left( \frac{1}{T_{ref}} - \frac{1}{T_{cell}} \right) \right]$$

## Conservation of Enthalpy

Exit quality: 
$$X = \frac{Cp_{liq} [T_{inlet} - T_{sat}(P_{tank})]}{H_{vap}}$$

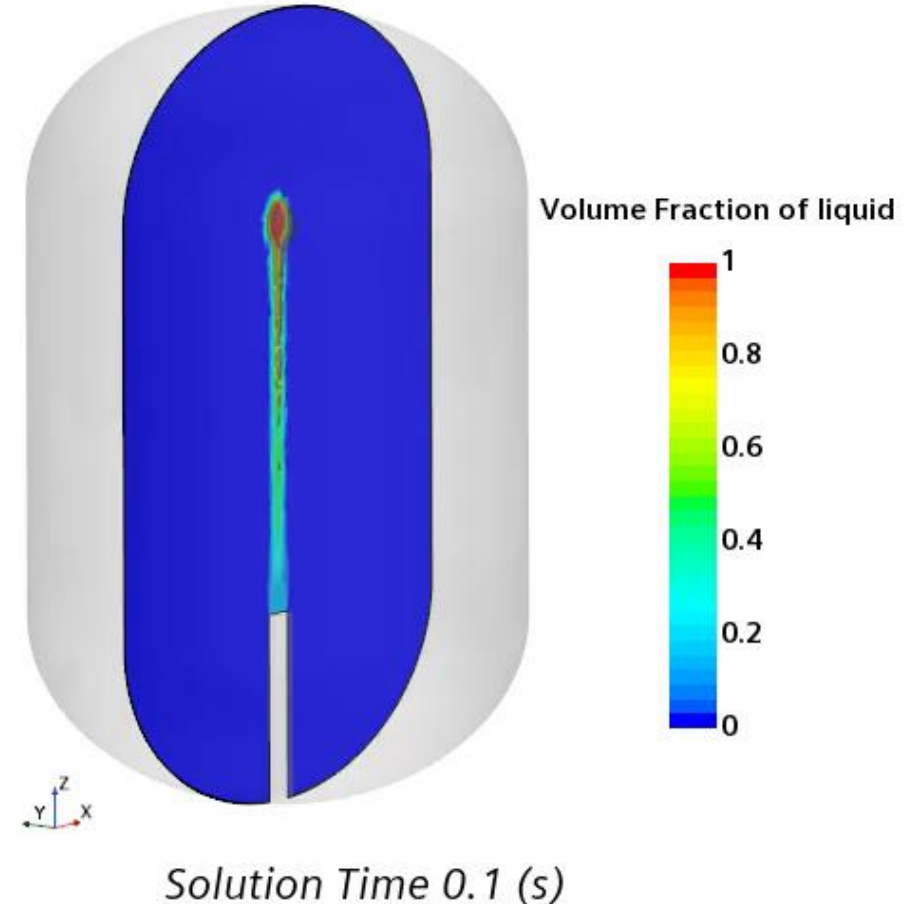
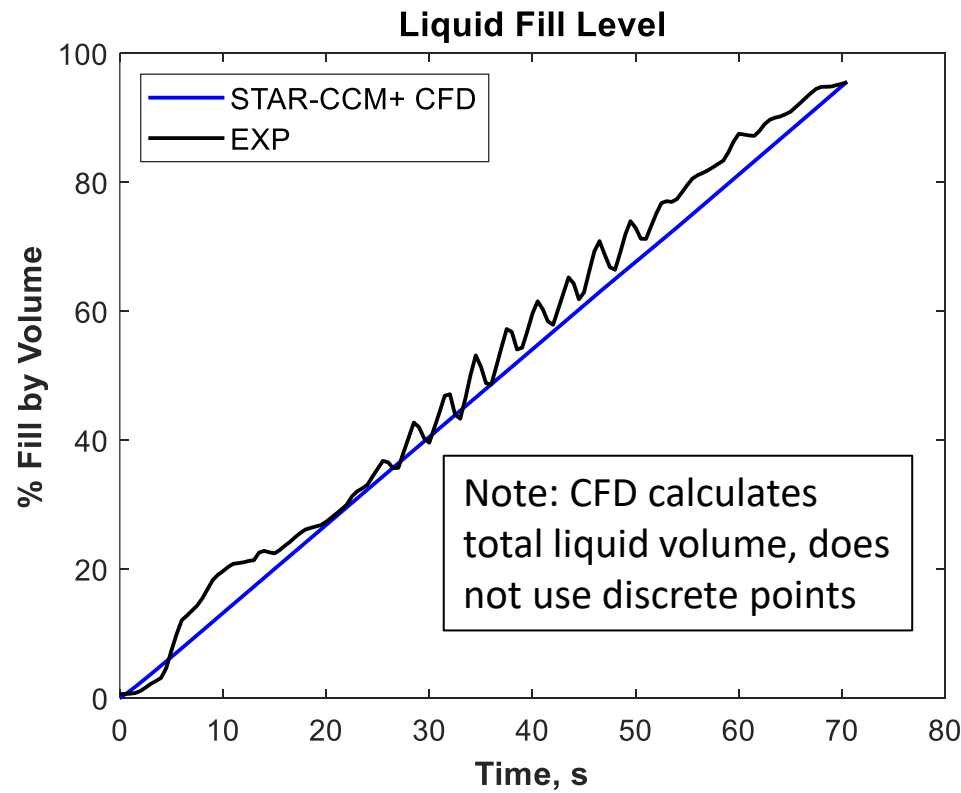
Void Fraction: 
$$\alpha_{vap} = \left[ 1 + \frac{1 - X}{X} \frac{\rho_{vap}}{\rho_{liq}} S \right]^{-1}$$

$S$  is the slip ratio (vapor velocity to liquid velocity) and is assumed to be 1.0

# Results: Fill Level Evolution



- Oscillations in the liquid fill level are observed during the middle section of the test shown on the plot due to discrete point sensors on the fill probe
- Upward liquid jet acted as a forced perturbation that excited the liquid-vapor interface inducing a slosh mode for that range of fill level
- CFD VOF model shows oscillations during exact time range (25-55 seconds)

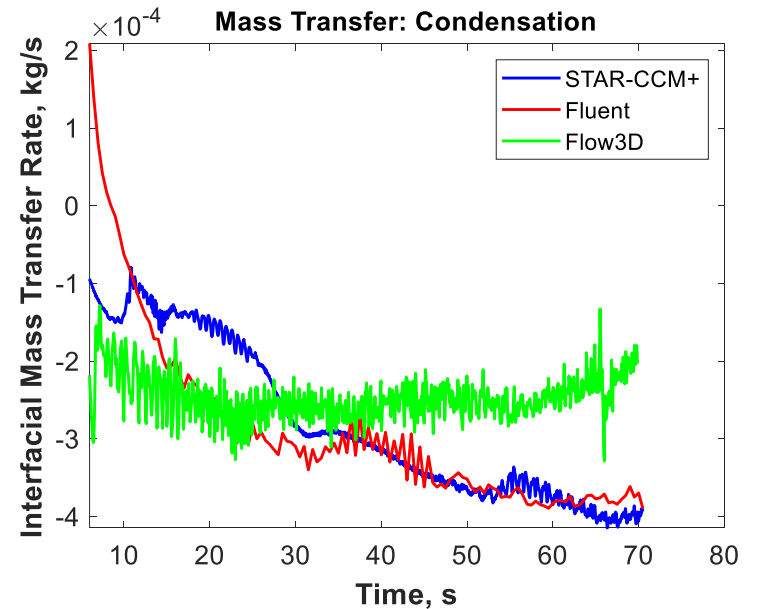
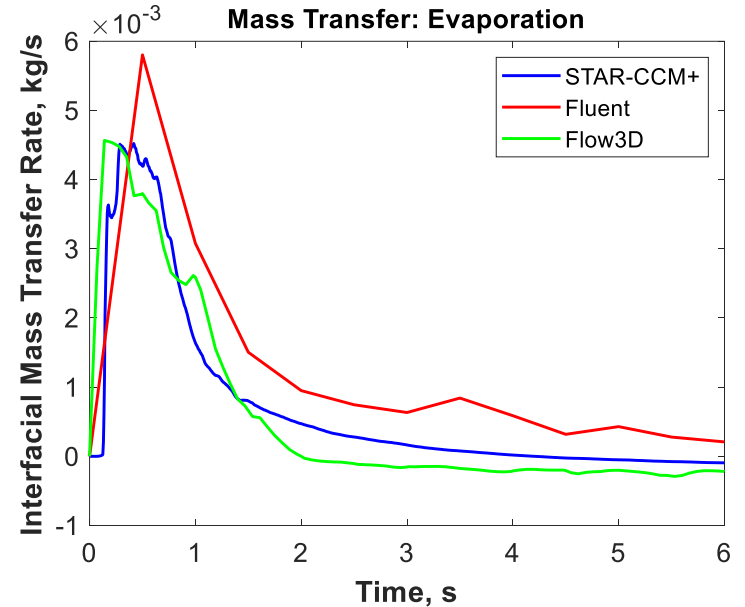
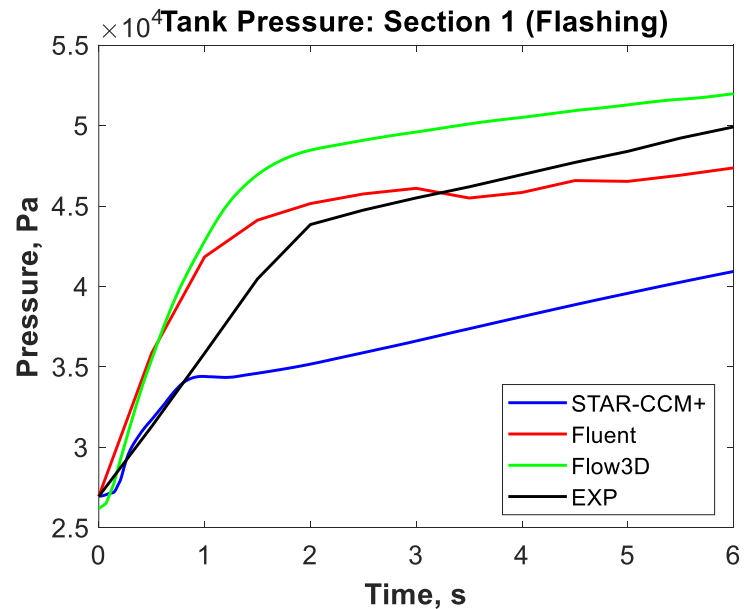
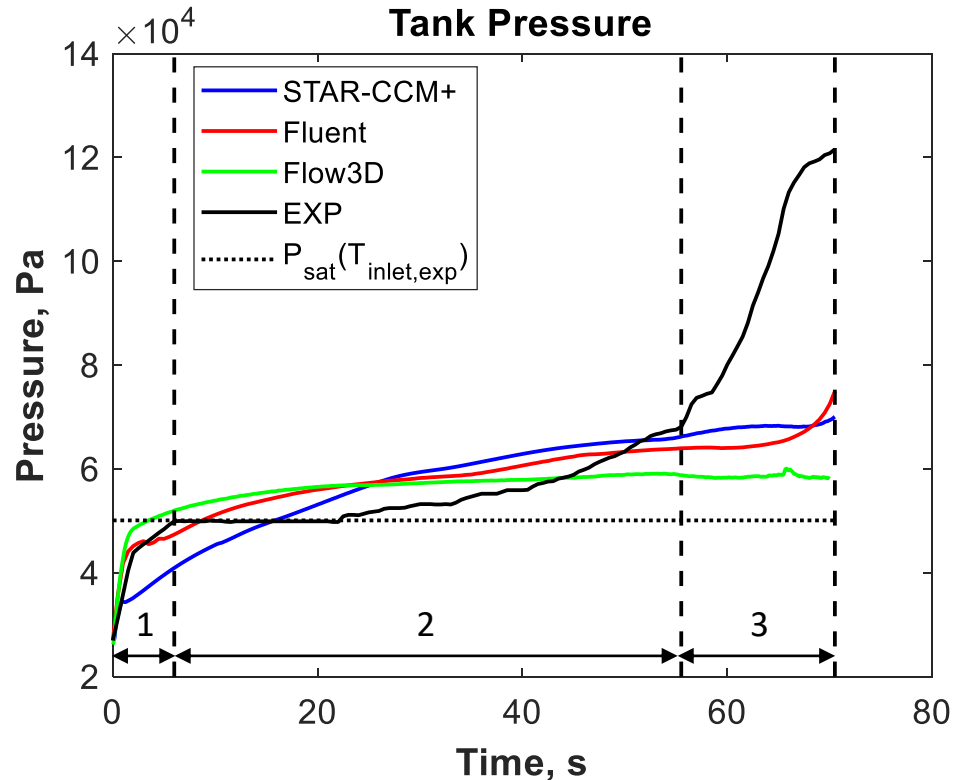


**Fill sequence of Volume Fraction on midplane and liquid surface using isosurface**



# Results: Pressure and Interfacial Mass Transfer

- The pressure response can be split into three sections:
  1. Flashing of inlet liquid; chardown of tank wall
  2. Ullage vapor condensation on liquid-vapor interface; continued vaporization
  3. Ullage compression
- STAR-CCM+ predicts a lower initial pressure rise due to lower evaporation interfacial mass transfer rate – related to phase distribution prediction during section 1: flashing of inlet liquid



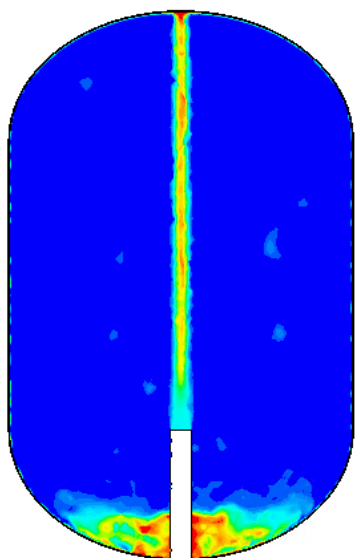


# Results: Phase Distribution

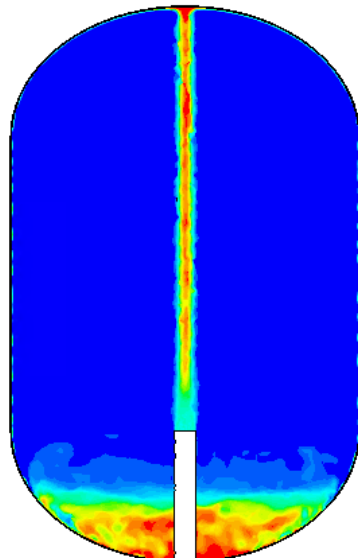


Volume Fraction of liquid  
0 0.2 0.4 0.6 0.8 1

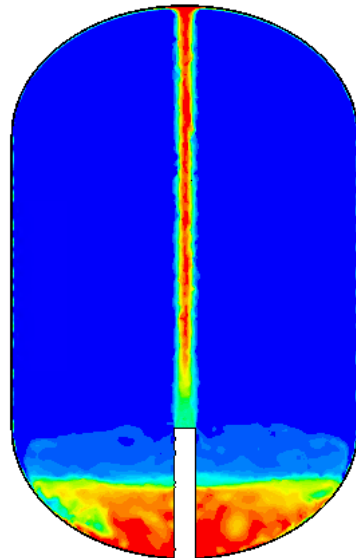
**STAR-CCM+**  
High-Resolution  
Interface Capturing  
Scheme



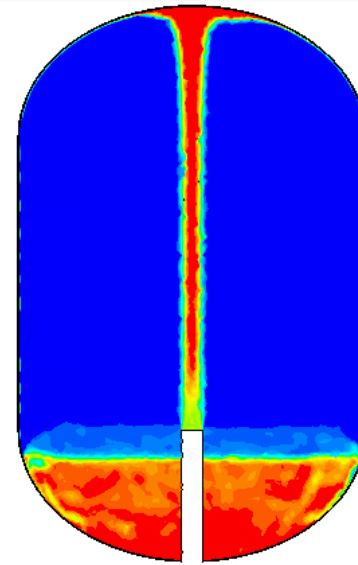
*Solution Time 2 (s)*



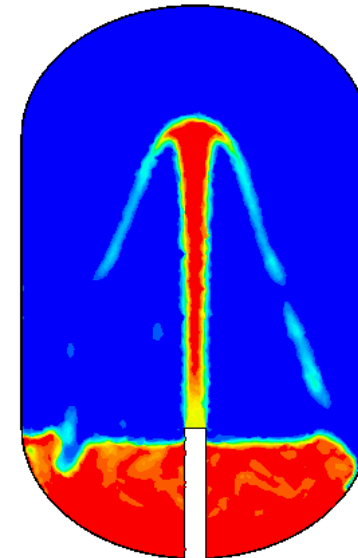
*Solution Time 4 (s)*



*Solution Time 6 (s)*



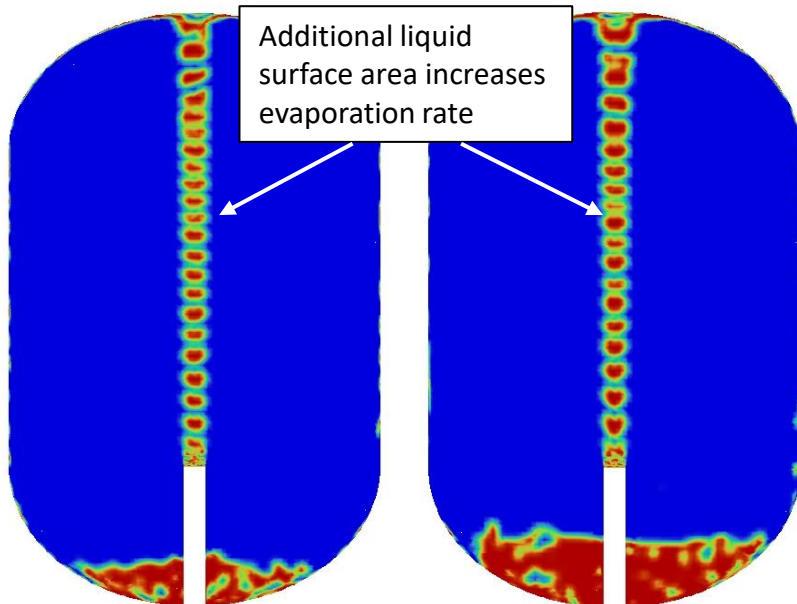
*Solution Time 10 (s)*



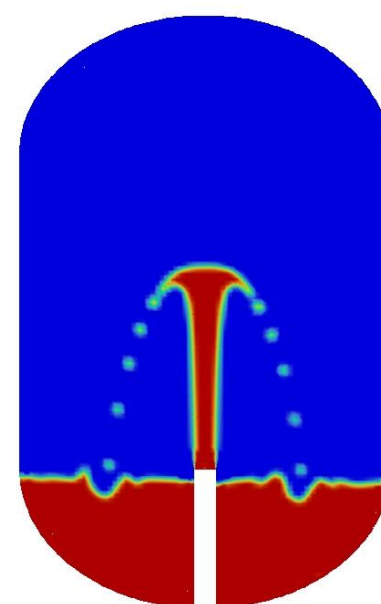
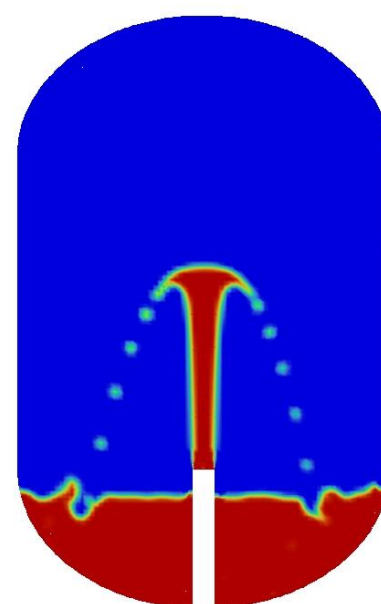
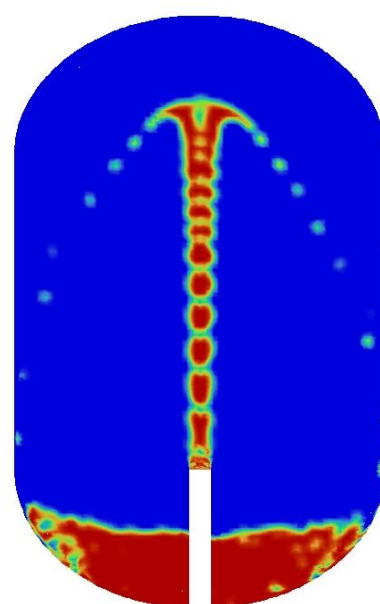
*Solution Time 12 (s)*

Volume Fraction of liquid  
0 0.2 0.4 0.6 0.8 1

**Fluent**  
Geometric  
Reconstruction  
(Explicit)



Additional liquid surface area increases evaporation rate

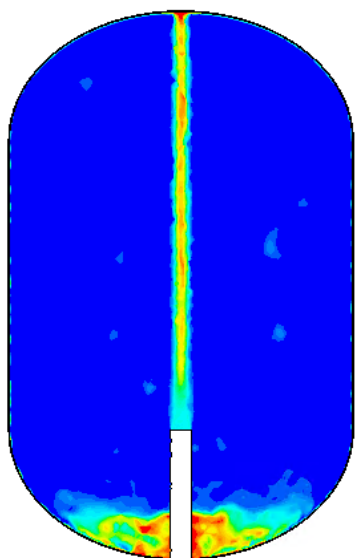


# Results: Phase Distribution

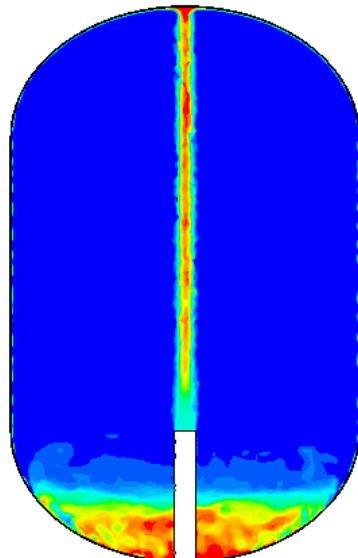


Volume Fraction of liquid  
0 0.2 0.4 0.6 0.8 1

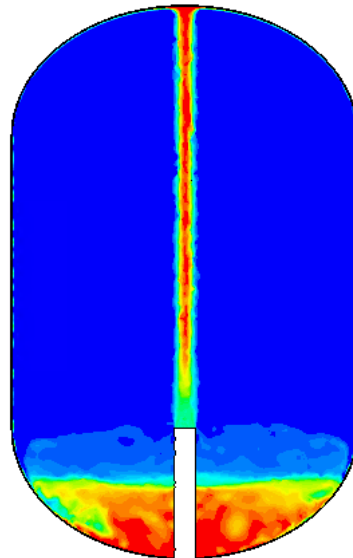
**STAR-CCM+**  
High-Resolution  
Interface Capturing  
Scheme



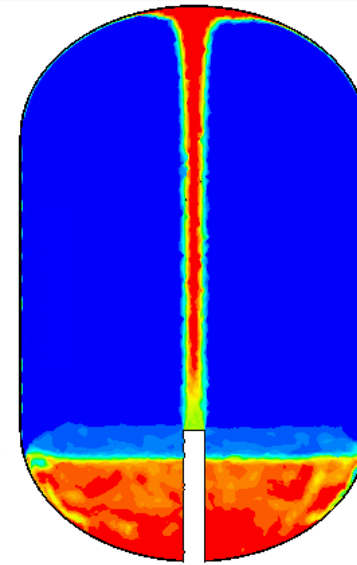
Solution Time 2 (s)



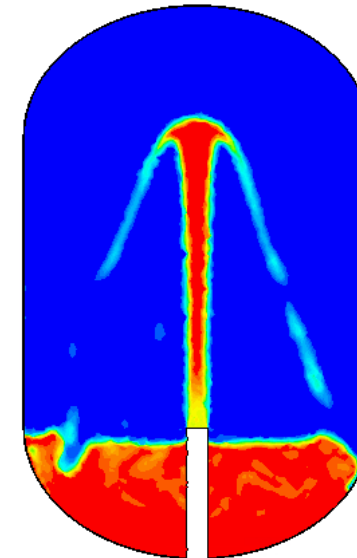
Solution Time 4 (s)



Solution Time 6 (s)



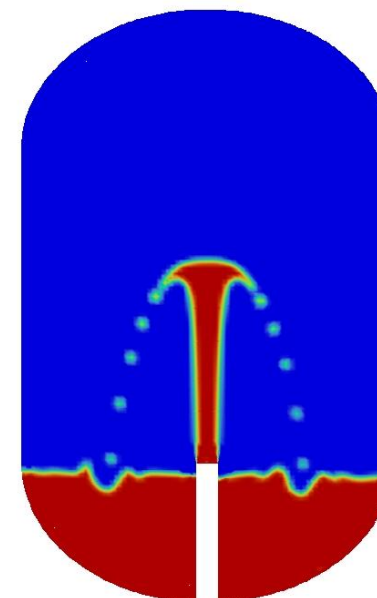
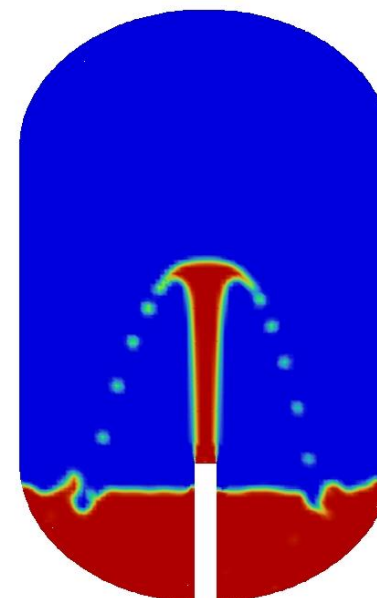
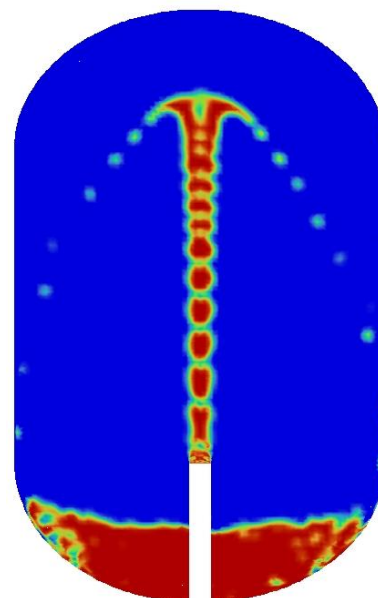
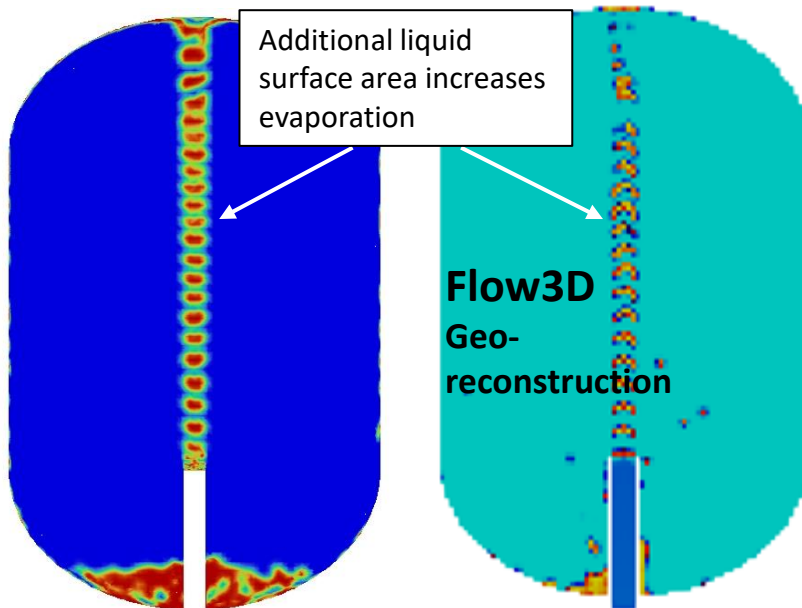
Solution Time 10 (s)



Solution Time 12 (s)

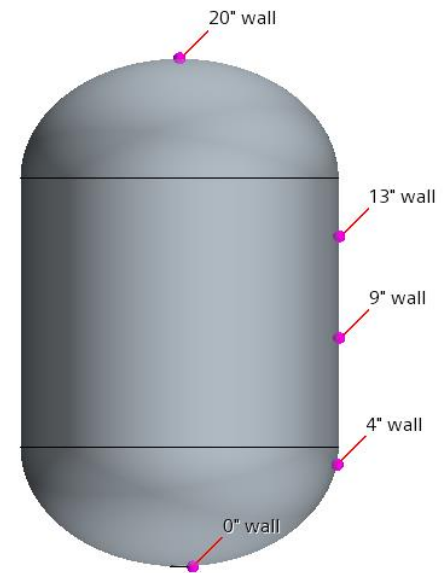
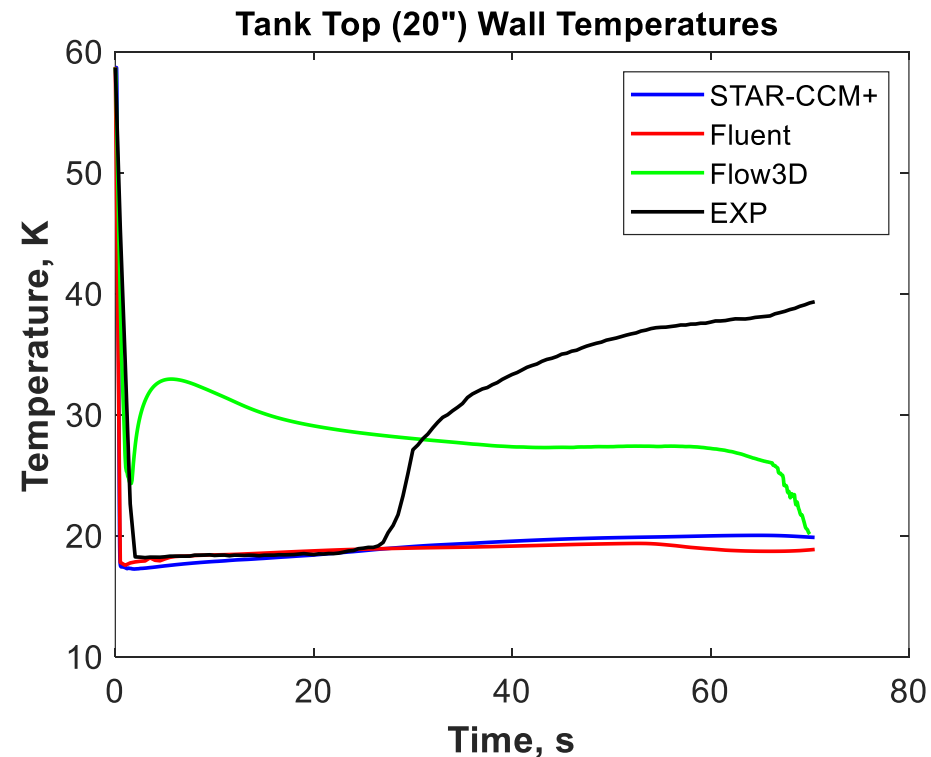
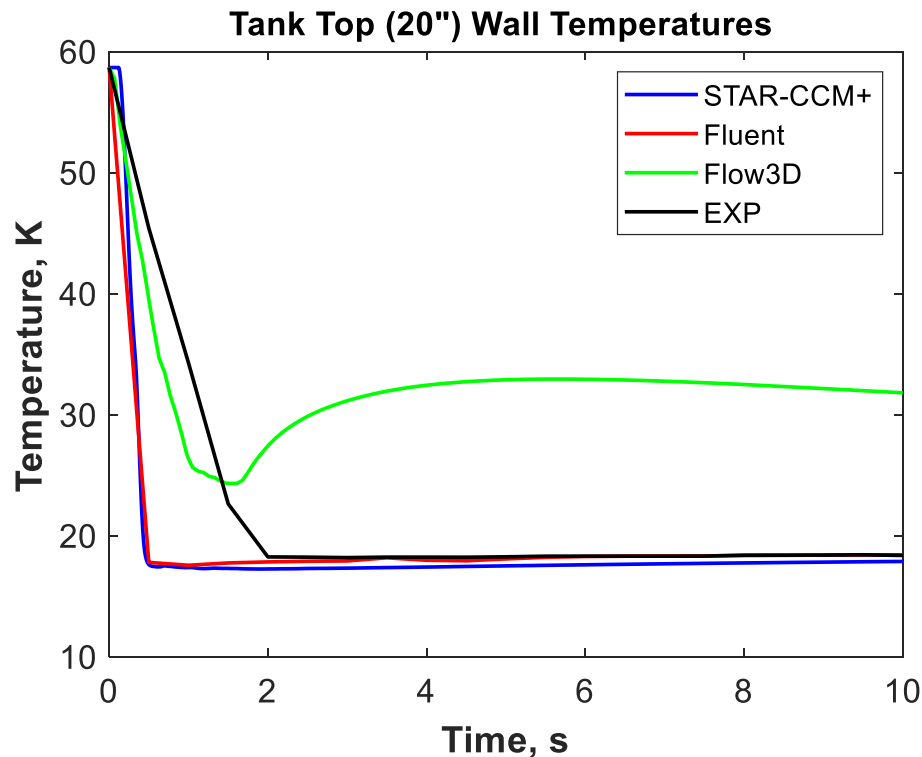
Volume Fraction of liquid  
0 0.2 0.4 0.6 0.8 1

**Fluent**  
Geometric  
Reconstruction  
(Explicit)



# Results: Top Wall Temperature Tank Chardown

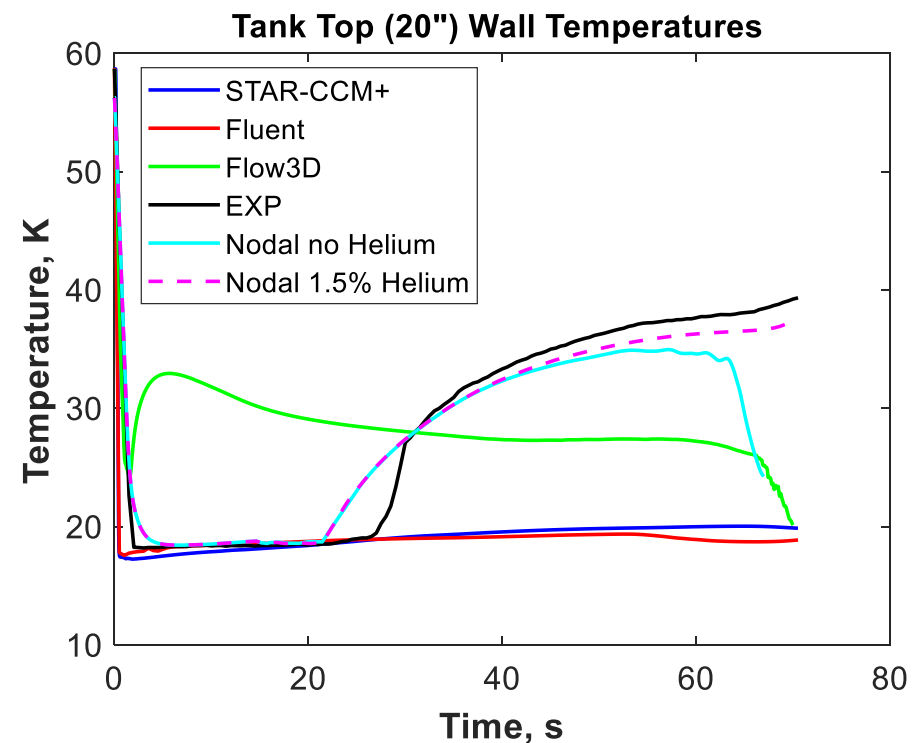
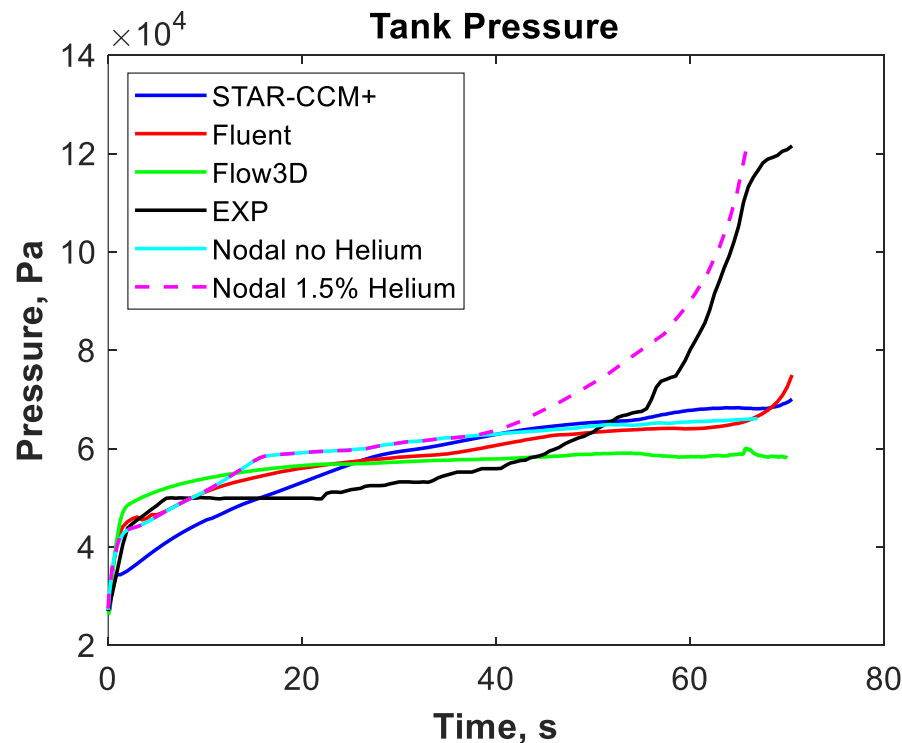
- Despite the differences in phase distribution early in the fill process, STAR-CCM+ and Fluent predict very similar chardown responses
- Flow3D pressure prediction exceeded  $P_{sat}(T_{inlet,exp})$  very quickly so the jet did not impinge on the top dome as long as Fluent and STAR-CCM+ predictions, yielding a higher temperature
- Late increase in experimental temp is assumed to be from heat leak that was unknown (instrumentation leads entering through top of tank)



# Presence of Helium



- None of the CFD cases considered accurately predicted the ullage compression/pressure rise near the end of the fill
- Helium gas used to purge system between tests may have become trapped in the tank and mitigated condensation near the end of the fill
- The effect of the presence of Helium on the pressure response was studied using a SINDA/FLUINT nodal model (B. Sakowski) which also included a 6W heat leak on the top dome
- Mass fraction of Helium was set to 1.5% and initially distributed in the bottom ullage nodes
- Case without Helium compares well to CFD while case with Helium compares well to experiment by capturing ullage compression and top wall temperature rise



- **Conclusions**

- All three codes predicted similar results; however, the Volume Fraction discretization schemes showed influenced on evaporation mass transfer rates and tank pressure
- None of the CFD cases considered accurately predicted the ullage compression/pressure rise near the end of the fill and may be due to the presence of Helium (consistent between STAR-CCM+, Flow3D, and Fluent)
- Nodal model with very low fraction of Helium was able to accurately capture the late pressure rise
- Modeling mass transfer with a non-condensable (e.g. Helium) needs maturation for accurate CFD predictions of cryogenic storage and transfer problems

- **Acknowledgments**

- The authors acknowledge and thank the Cryogenic Fluid Management Modeling Portfolio and Cryogenic Fluid Management Portfolio Project for funding this work. The authors also recognize Matthew Moran for his insight on the experimental setup and data analysis.



**BACKUP**

# Experimental Overview (2 of 2)



- Experimental Measurements Taken:

- Tank Pressure
- Fluid Temperatures
- Solid Wall Temperatures
- Fill Level
- Mass Flow Rate
- Inlet Temperature

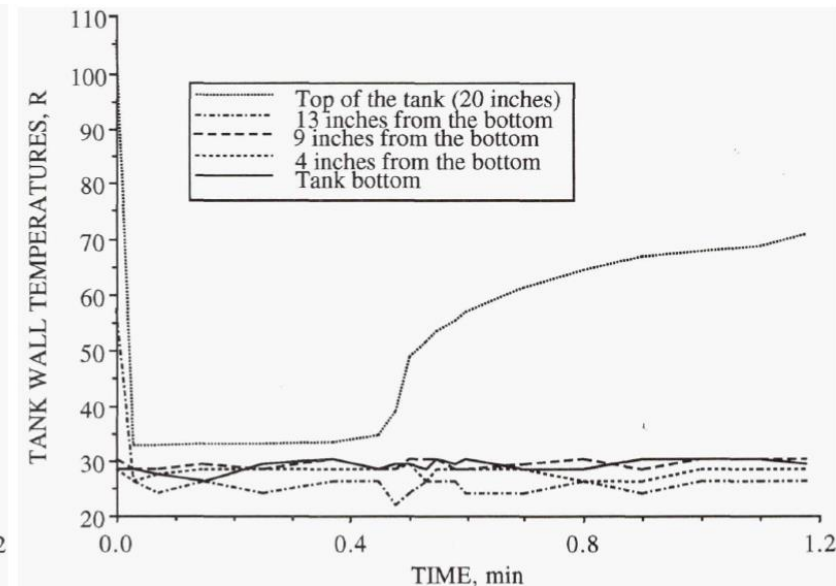
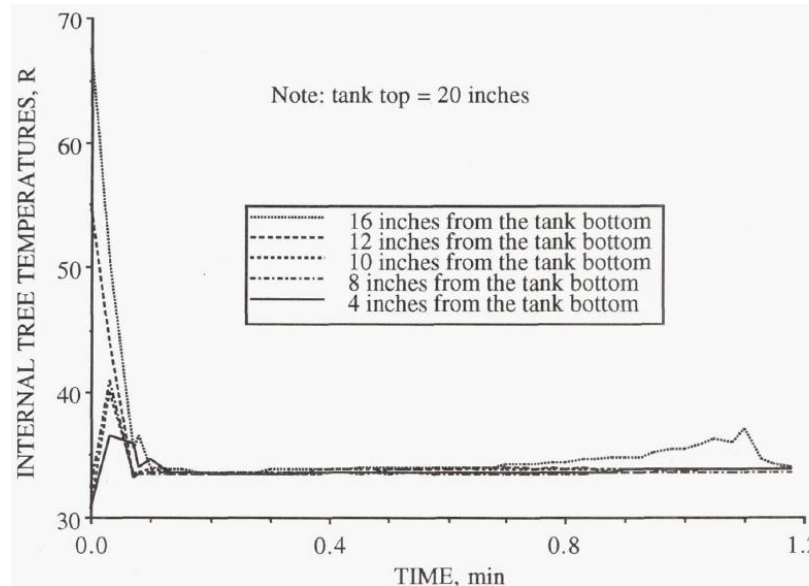
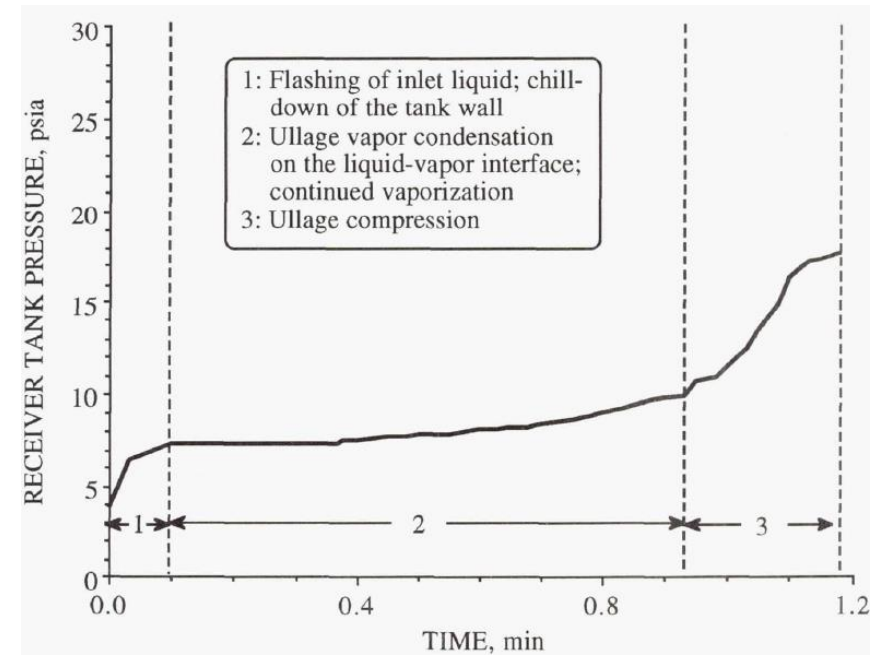
Reported as  $f(t)$

Reported as  $\overline{f(t)}$

Measured Test Quantities for Test Number 9093G (NASA TM-105273, 1991)

Fill Config	Inlet Venturi Temp K	Inlet Venturi Flow Rate kg/s	Initial Tank Pressure psia	Final Fill Level % by volume
Upward Pipe	18.55	0.034	3.8	96

↳  $P_{sat}(T_{inlet}) \approx 8.2$  psia



Data reported for upward pipe configuration (NASA TM-105273, 1991)

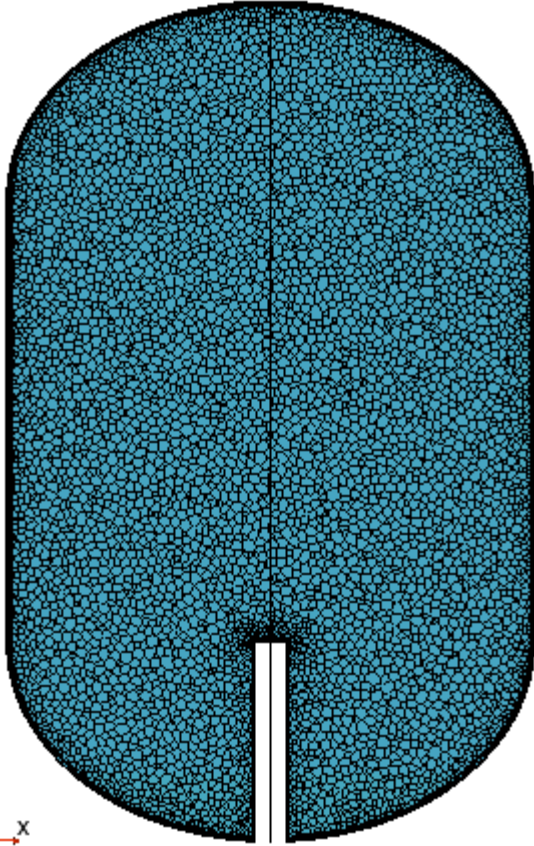
- Due to the amount of uncertainty in the experiment, several sensitivity studies were considered
  - Inlet Condition and Mass Transfer
  - Inlet Temperature
  - Accommodation Coefficient
  - Geometric Configuration and Wall Thickness
  - Presence of Helium
- Note: Each simulation was run until the predicted pressure reached the final pressure in the experiment (as opposed to the fill level)
- This allows us to assess the CFD model's capability of predicting the tank pressure at the corresponding fill level
- In practice, it would be highly desirable for CFD models to accurately predict the following:
  - At what fill level would the transfer fail?
  - At what fill level would the receiver tank reach the MEOP?
  - Or for a successful transfer, what the pressure would be at the end of the transfer?



# Mesh Independence Study (1 of 2)

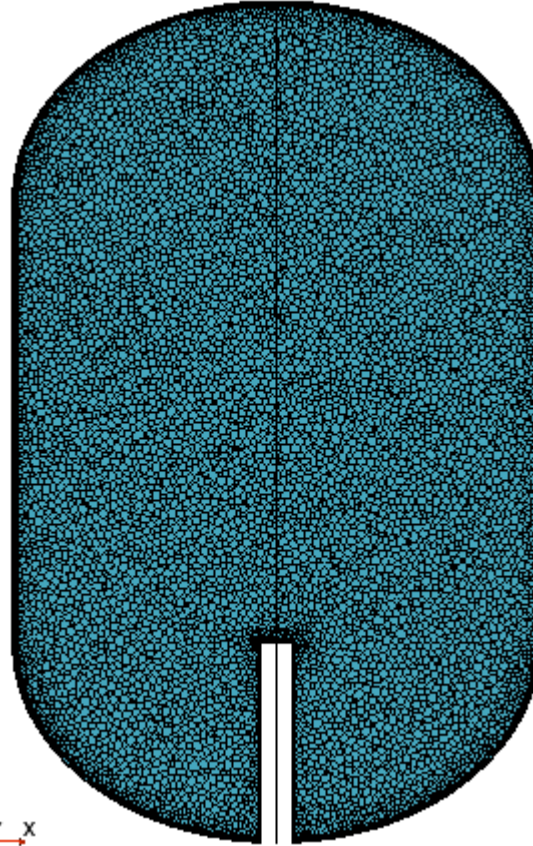


Coarse



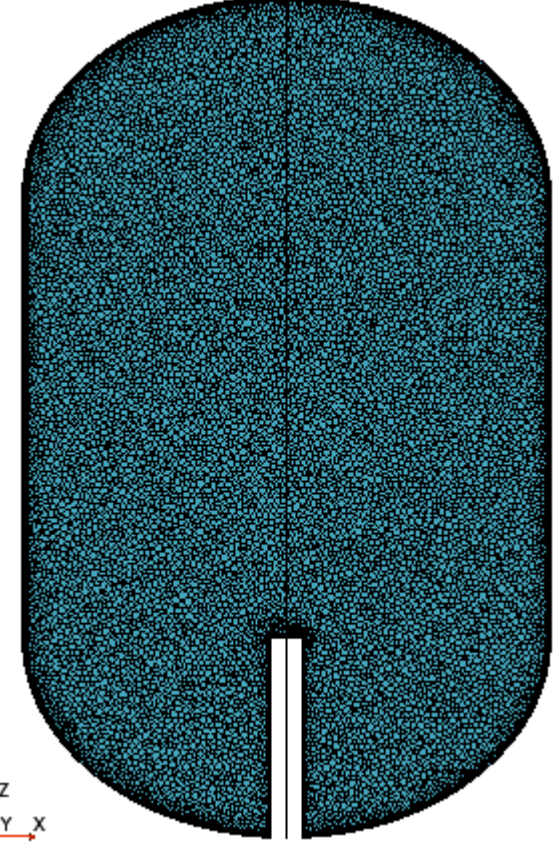
Medium base size \*  $(2)^{(1/3)}$   
0.77 million cells

Medium



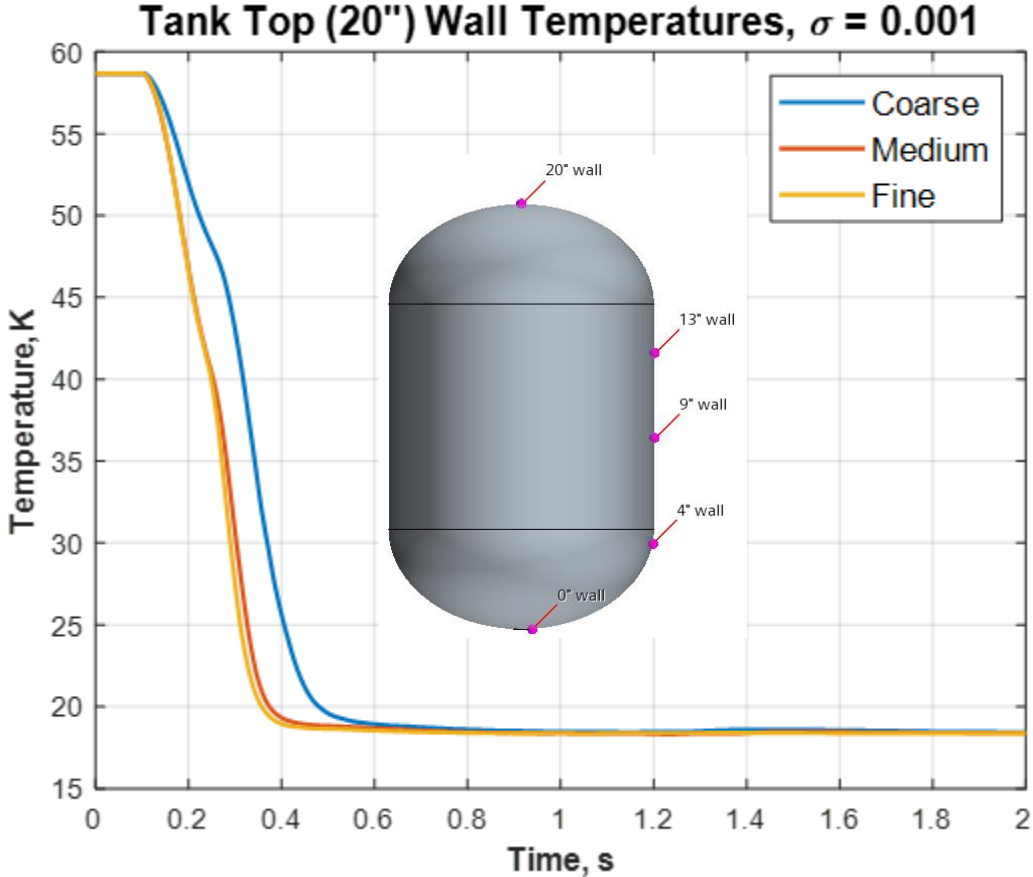
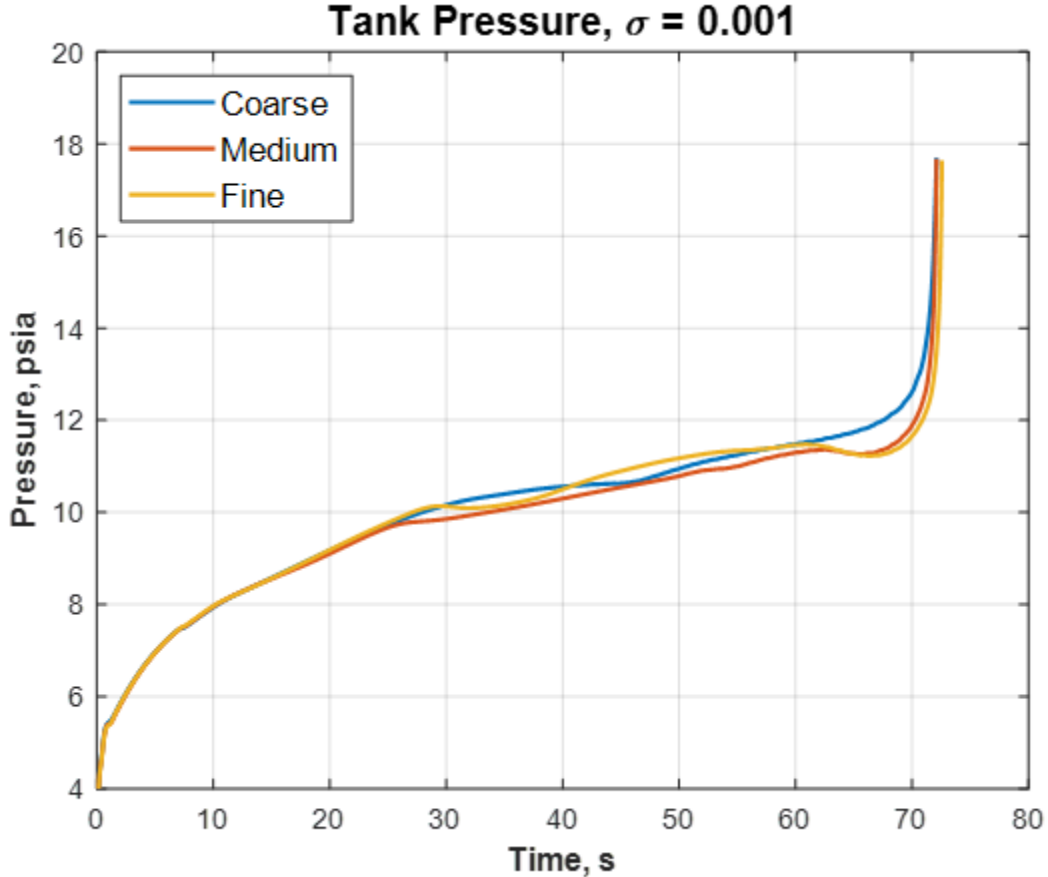
Medium base size = 4 mm  
1.47 million cells

Fine



Medium base size /  $(2)^{(1/3)}$   
2.32 million cells

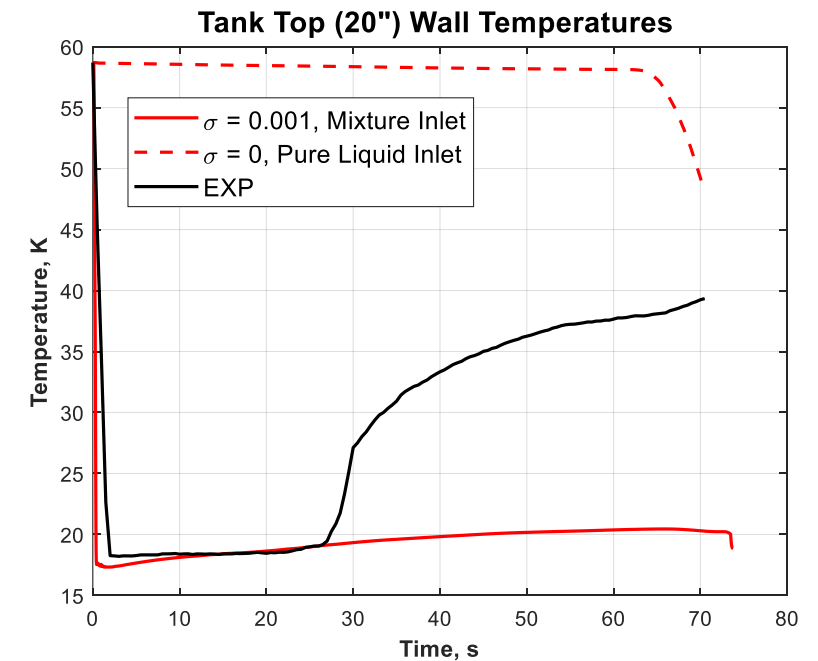
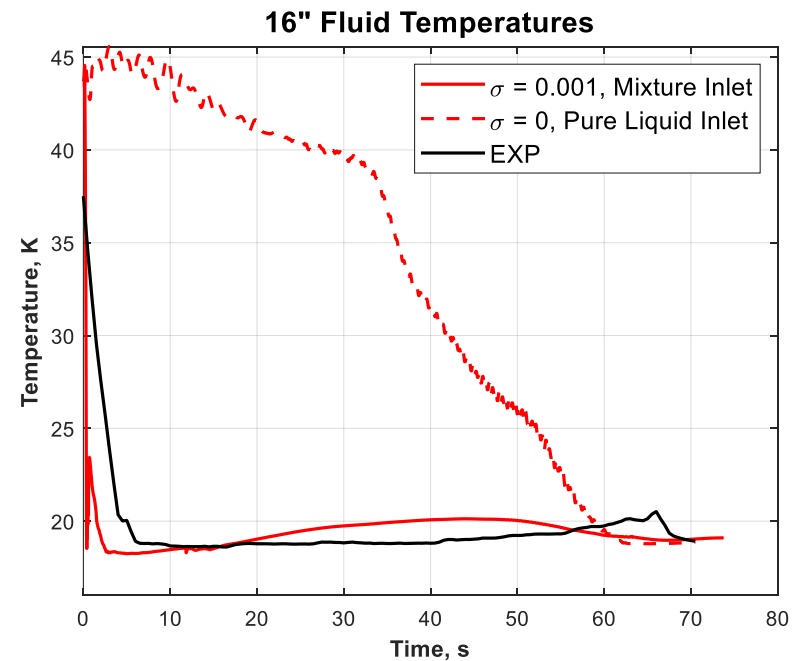
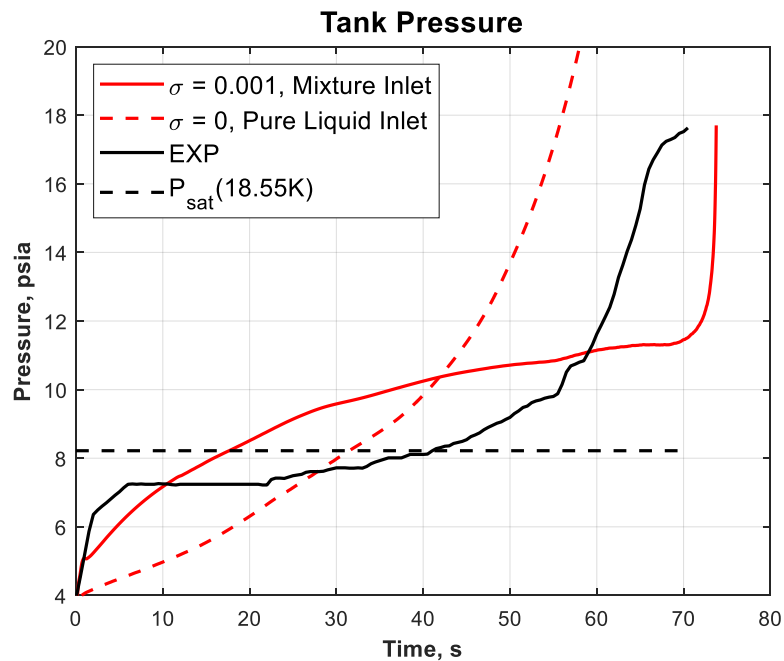
# Mesh Independence Study (2 of 2)



# Effect of Inlet Condition and Mass Transfer (1 of 2)

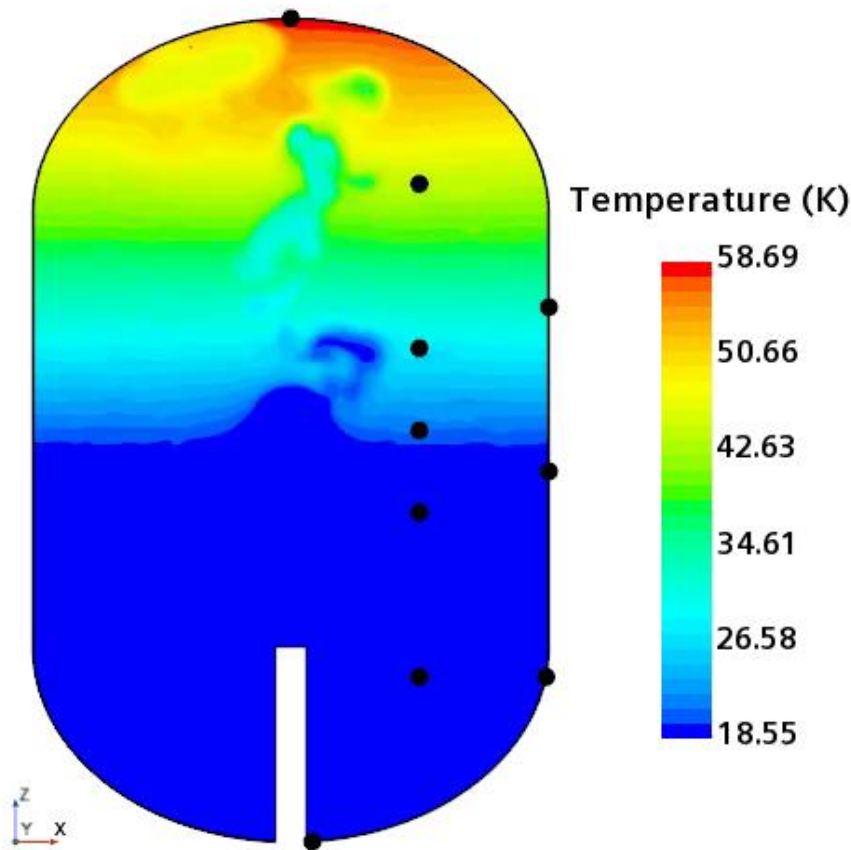


- First, a baseline case was compared to a case that implemented a pure liquid inlet (no flashing) and neglected interfacial mass transfer
- The baseline case (mixture inlet) predicts the tank pressure and temperature responses with better accuracy
  - Combination of injecting two-phase flow and evaporation yields a larger initial pressure rise
  - Later in the fill, the Pure Liquid Inlet case predicts large pressure rise due to ullage compression while condensation dominates in baseline case keeping pressure low
  - Temperature response is predicted well with 'mixture' inlet due to higher velocity jet penetrating to top of tank chilling probes and inducing mixing



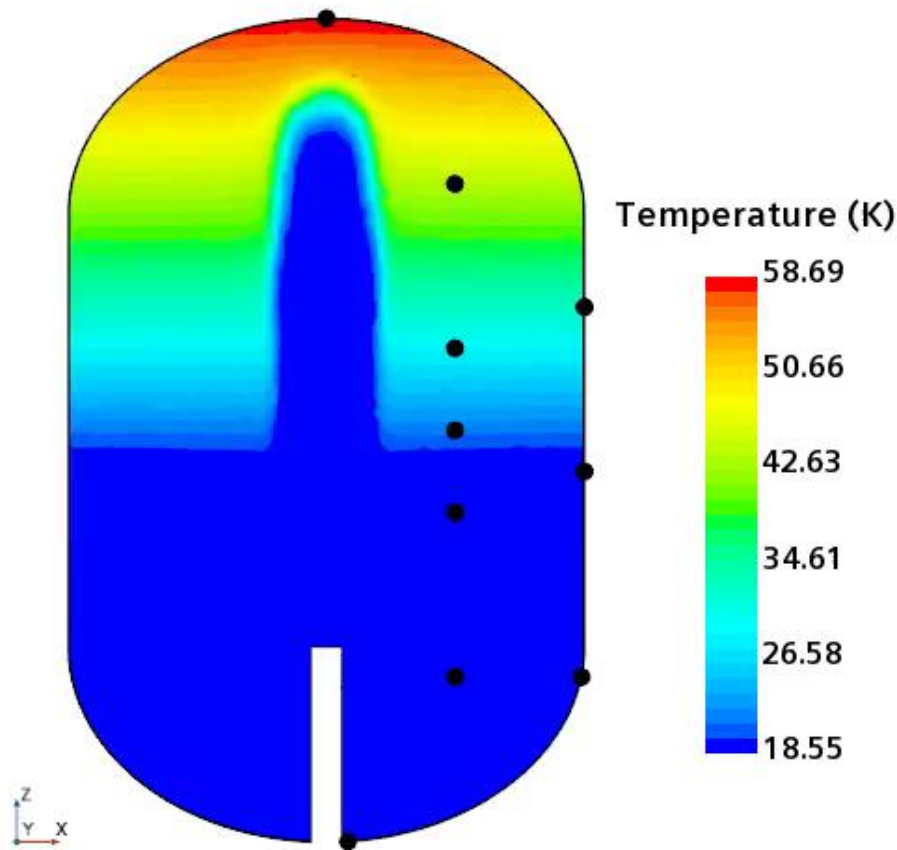


## Pure Liquid Inlet



Solution Time 0.2 (s)

## Mixture Inlet

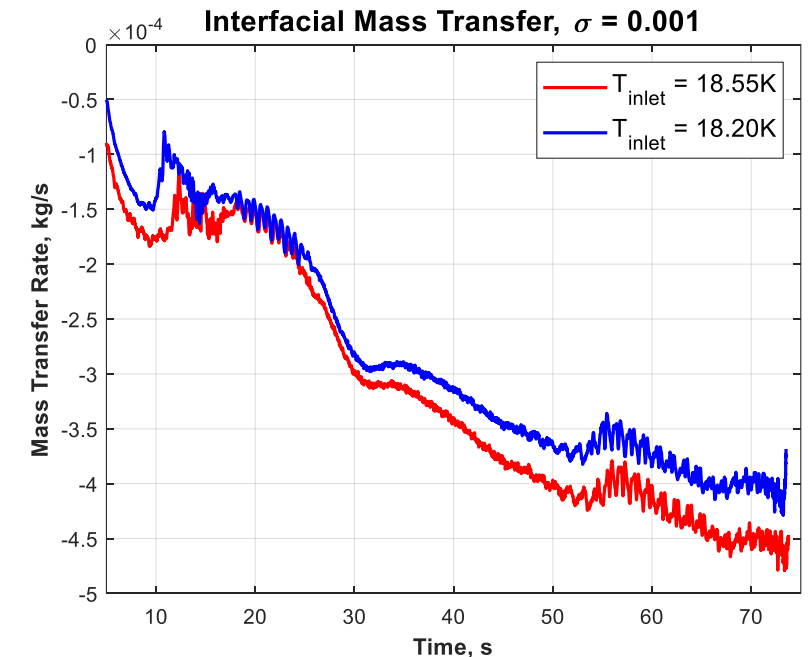
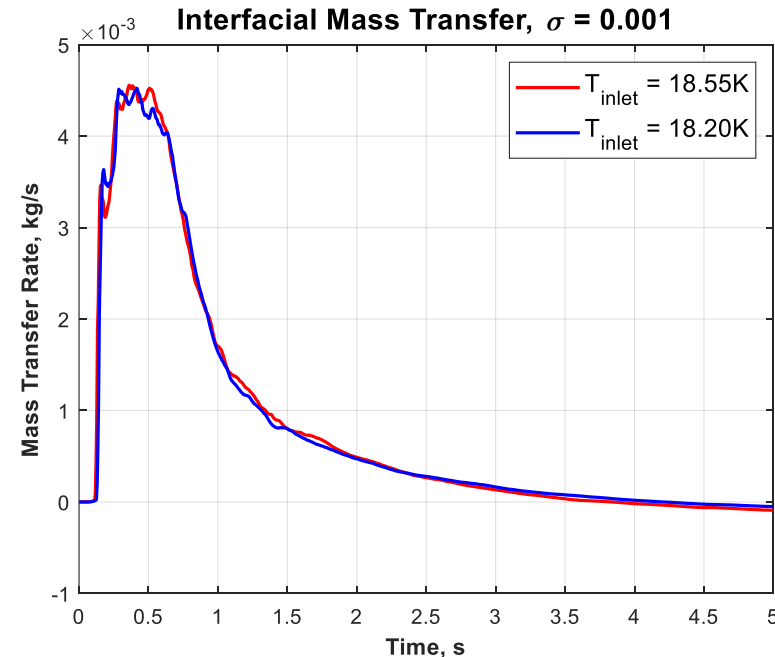
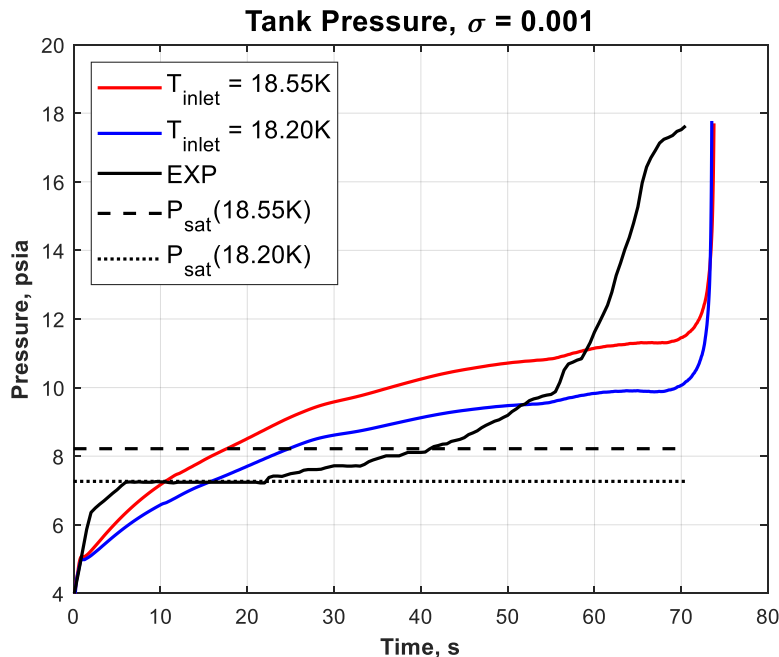


Solution Time 0.1 (s)

# Effect of Inlet Temperature



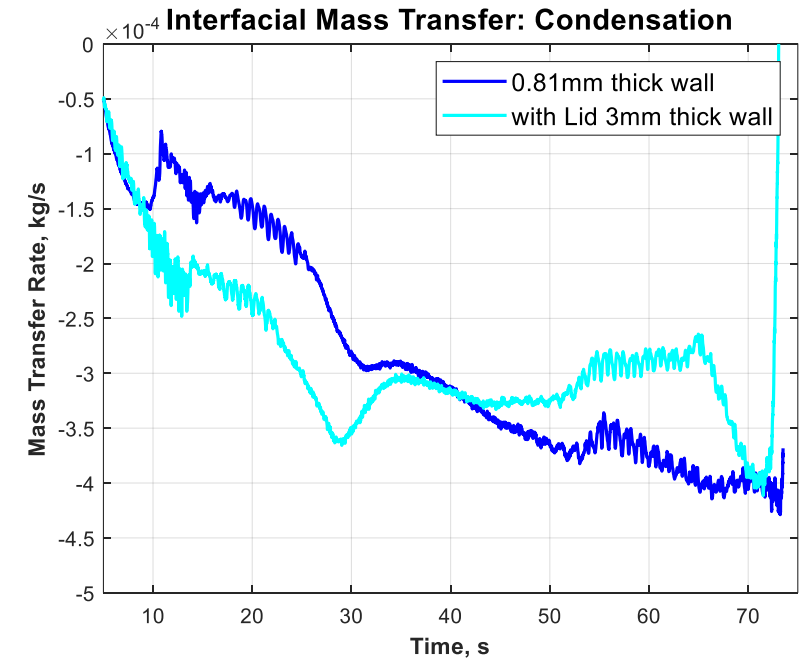
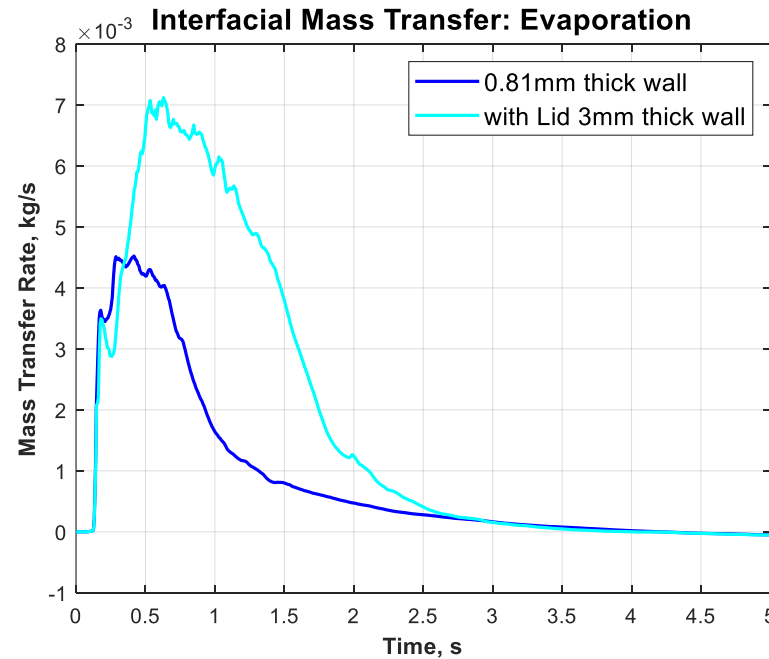
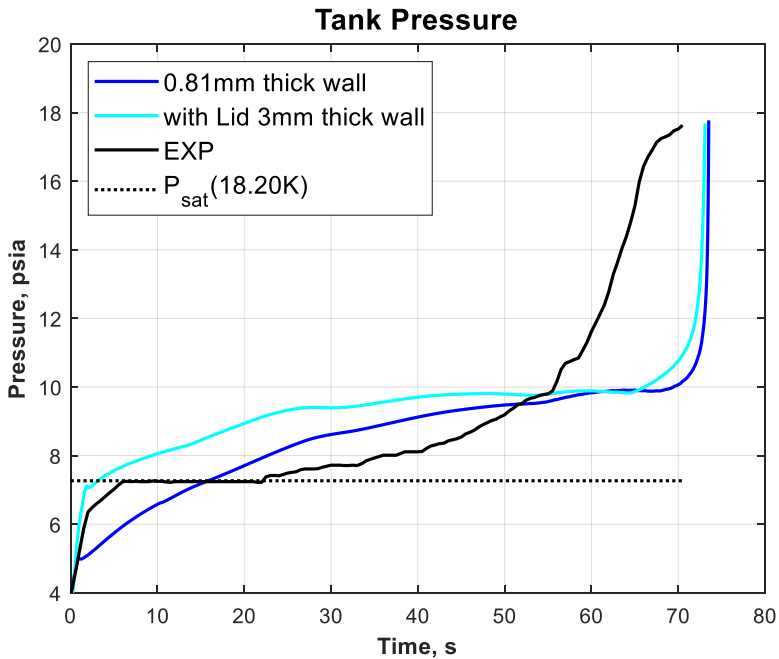
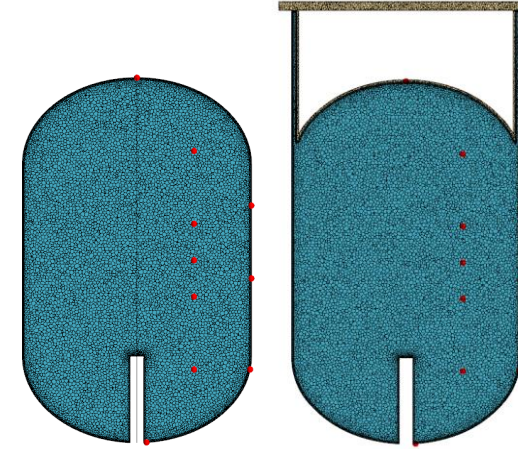
- Two “final” inlet temperatures of 18.20 and 18.55 K were considered
  - Measurement uncertainty
  - Experimental tank pressure quickly levels off at value very close to saturation pressure at 18.2 K
- Both cases under-predict initial pressure rise, over-predict middle section, and fail to predict ullage compression until extremely high fill levels
  - Condensation is over-predicted near end of fill
  - Predicted final fill level = 99.6% vs. Experiment final fill level = 96%
- Identical evaporation rates, higher temp yields higher condensation rate due to higher pressure



# Effect of Geometric Configuration (1 of 4)



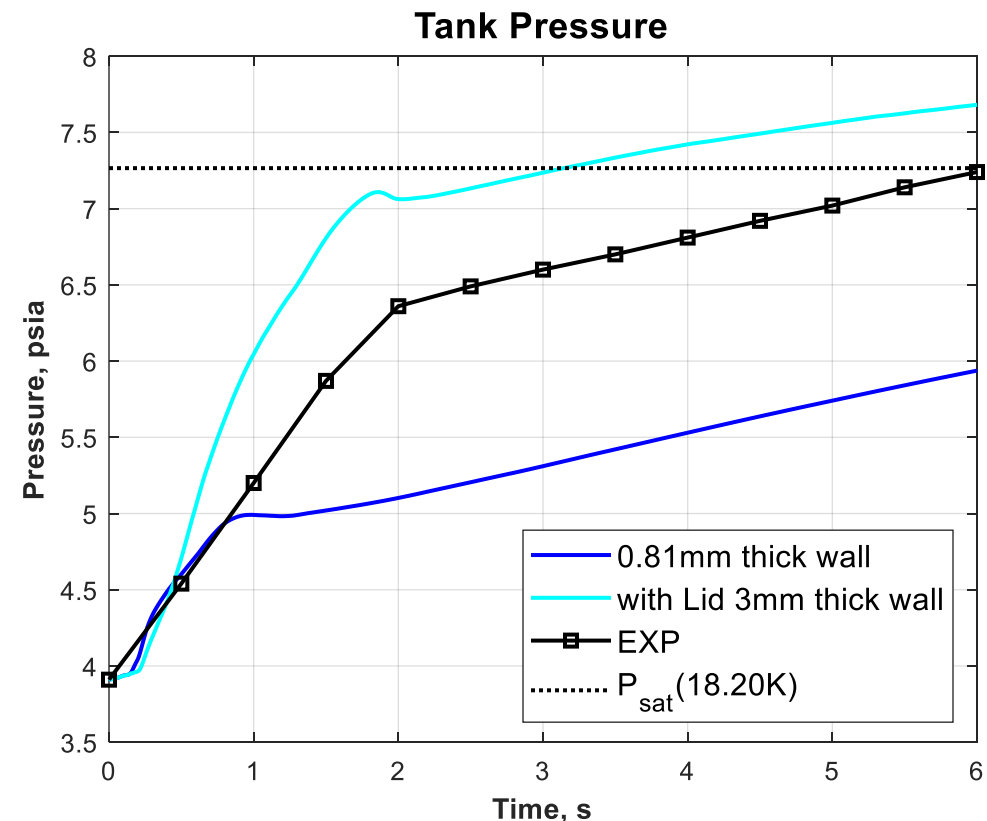
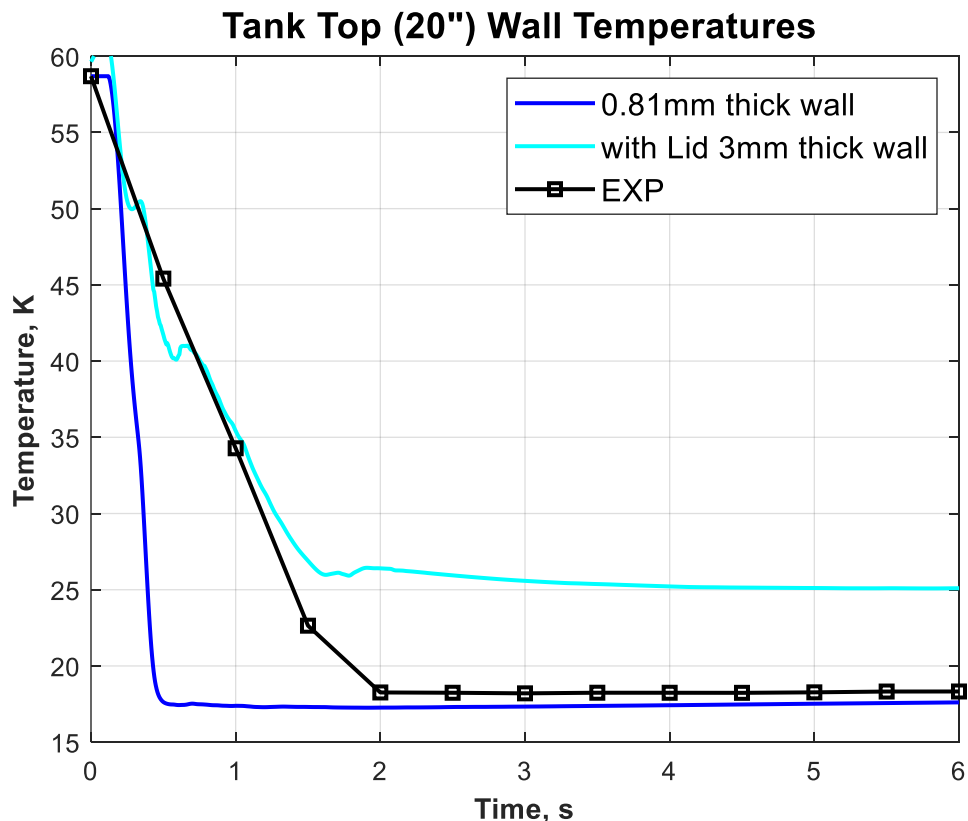
- Configuration with lid and thicker walls predicts higher pressure rise due to higher evaporation rate
- Thicker walls increased the thermal mass which extracts more energy from the walls during chilldown resulting in a higher pressure
- Since the two configurations bound the experimental pressure during the initial part of the fill, actual tank wall thickness may be somewhere between



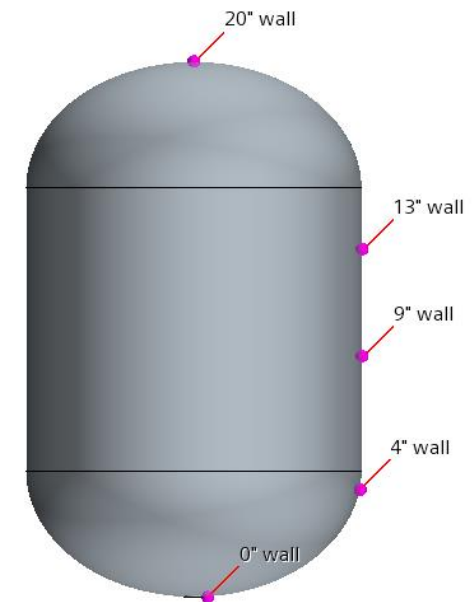
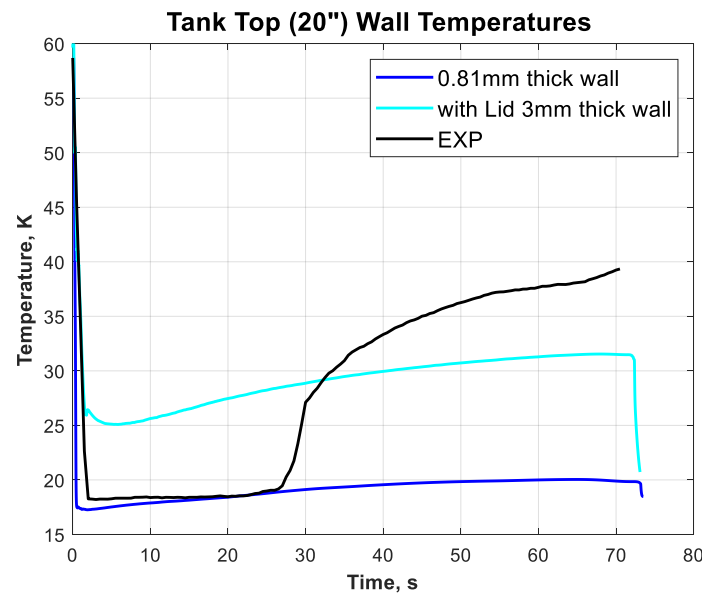
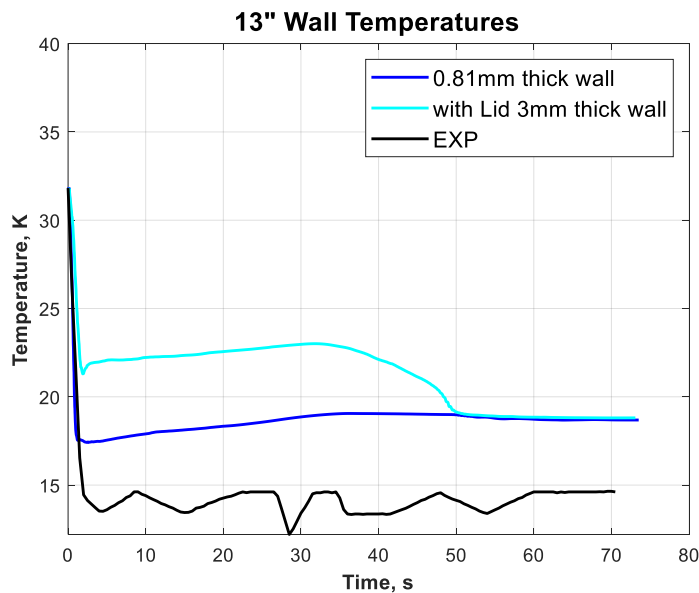
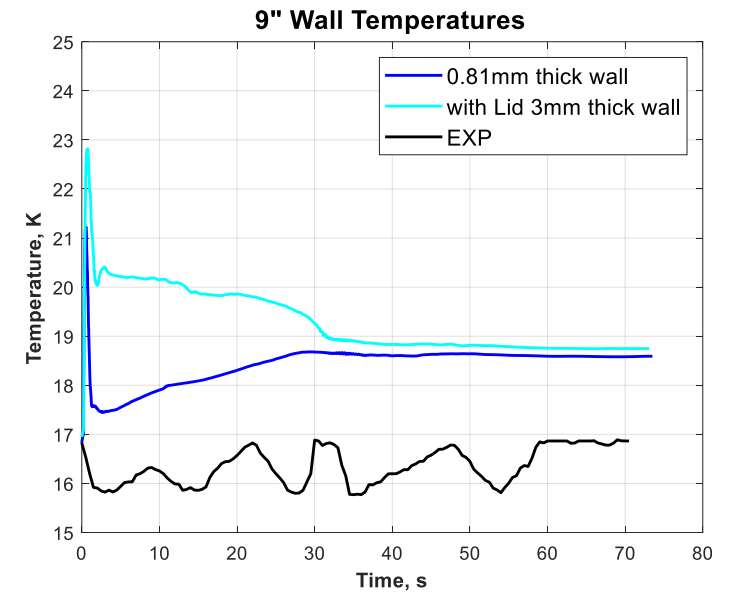
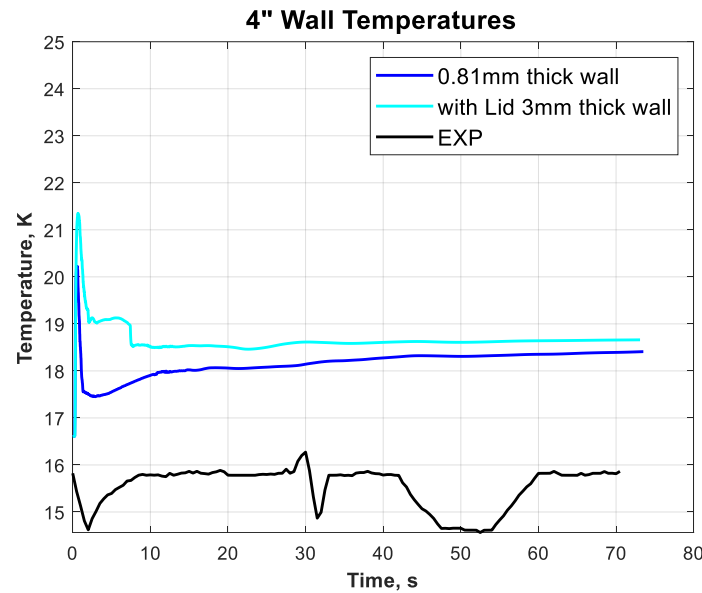
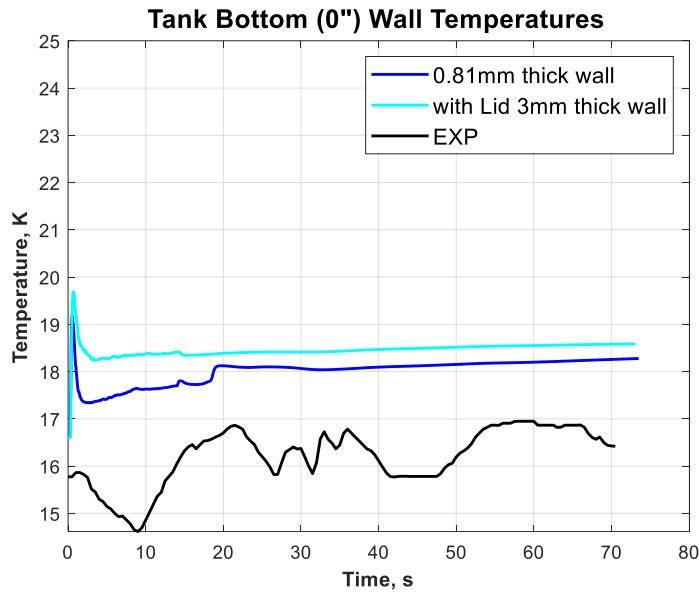
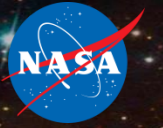
# Effect of Geometric Configuration (2 of 4)



- The chardown of the top wall temperature probe corresponds to a change in the pressure rise slope
- Once the probe is chilled down to the inlet temperature, the evaporation rate significantly diminishes yielding a slower pressure rise
- The thicker wall configuration doesn't chill all the way down to the inlet temp because it over-predicts the pressure rise so that the liquid jet no longer impinges on the top dome

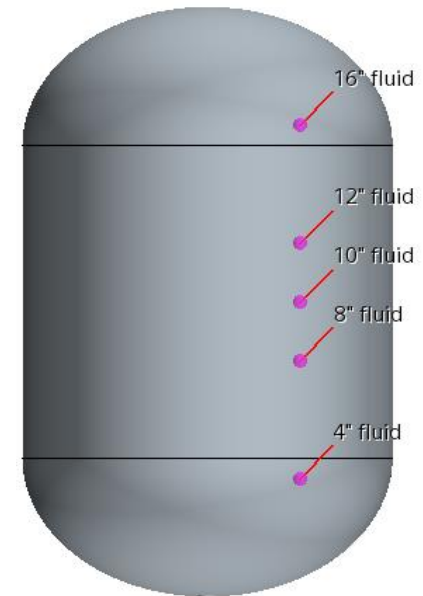
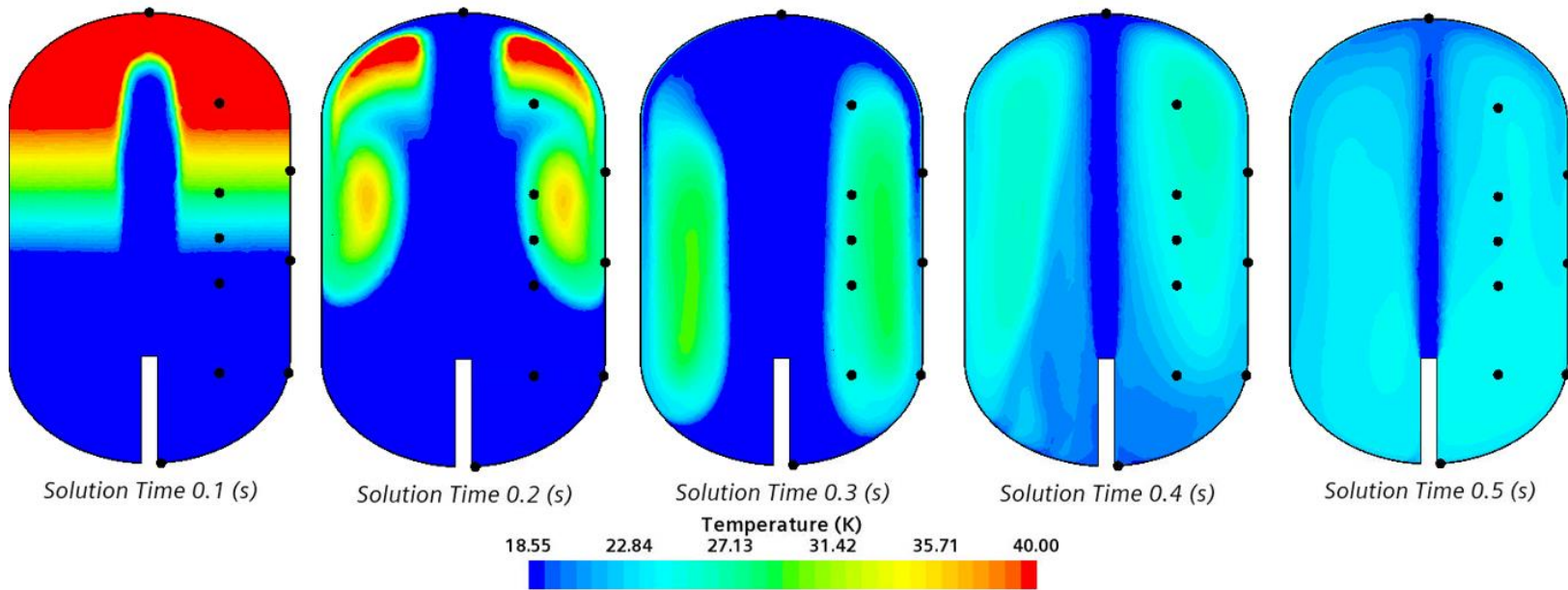
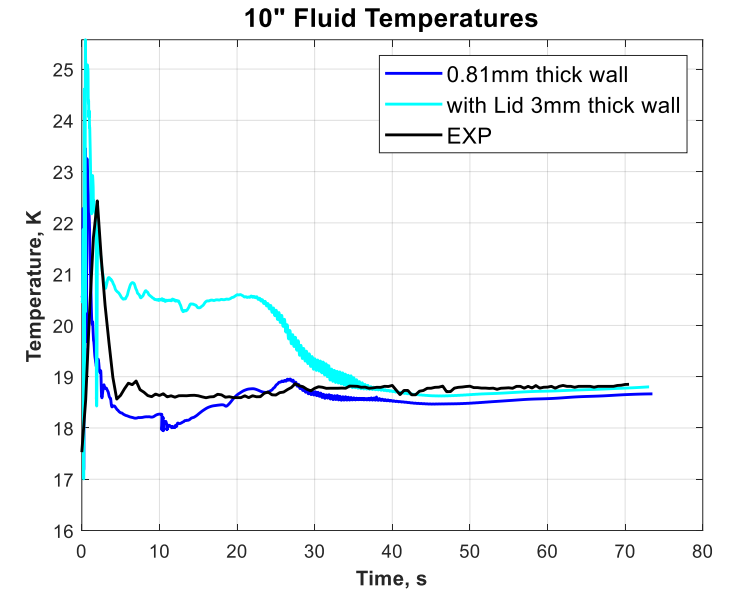
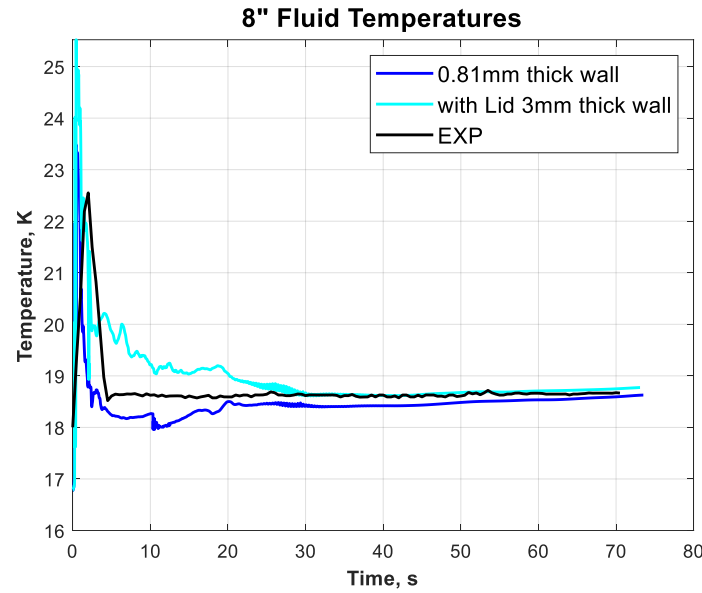
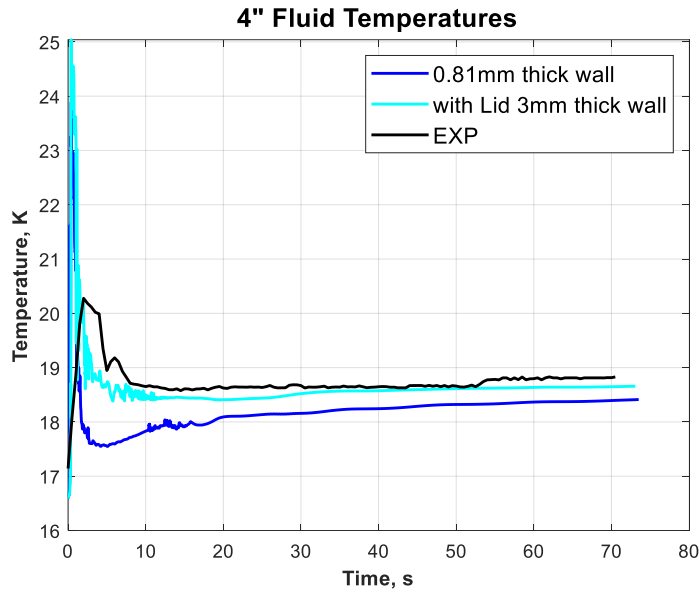
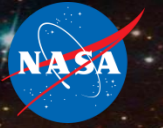


# Effect of Geometric Configuration (3 of 4): Wall Temperatures

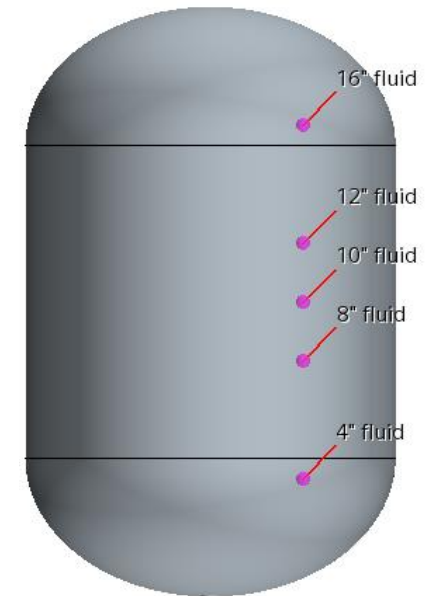
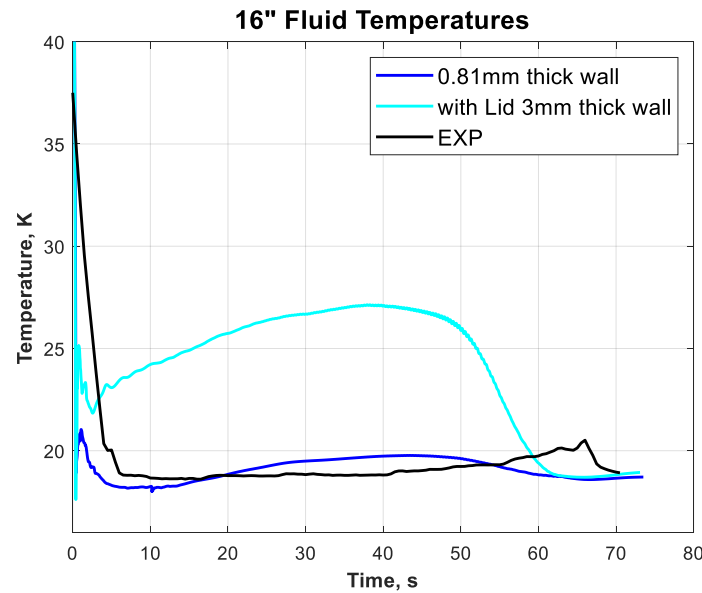
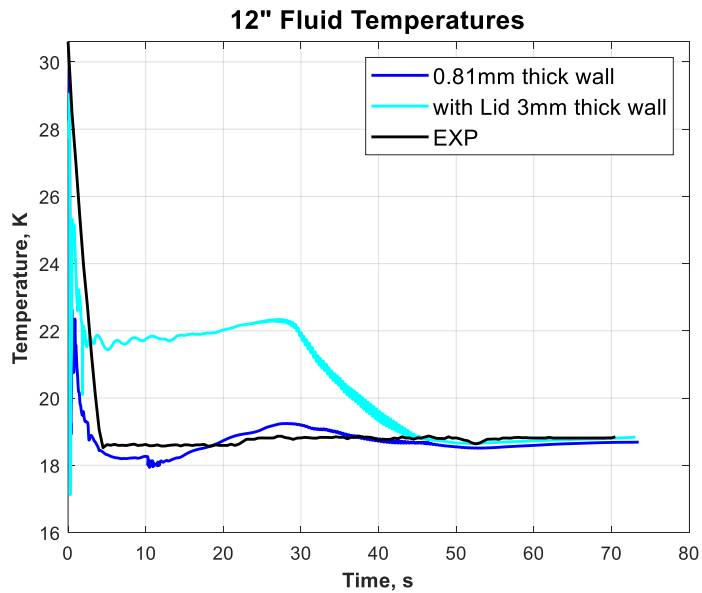
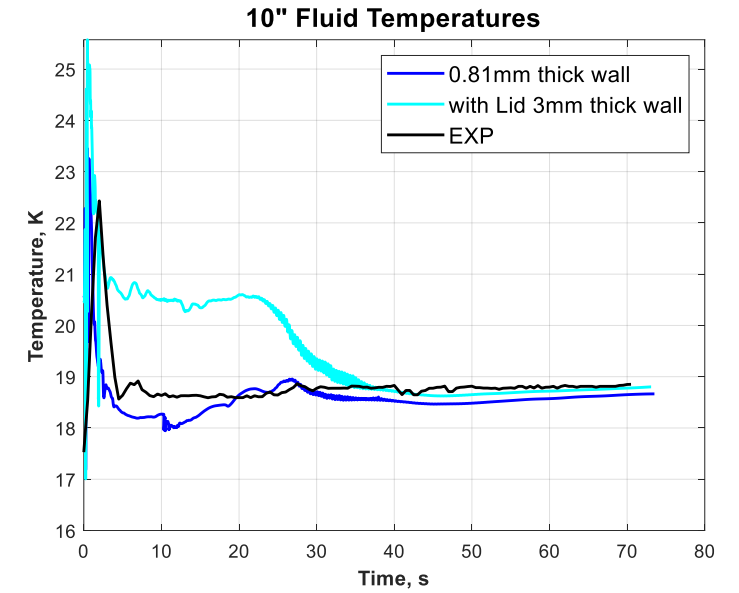
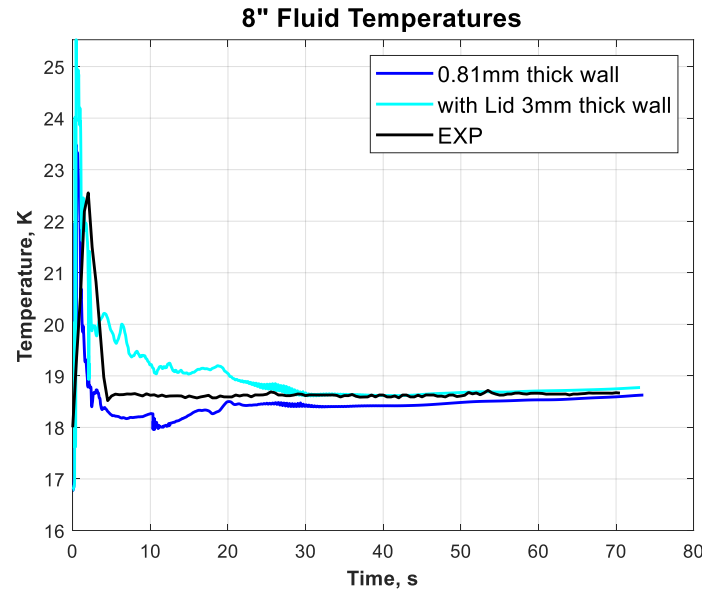
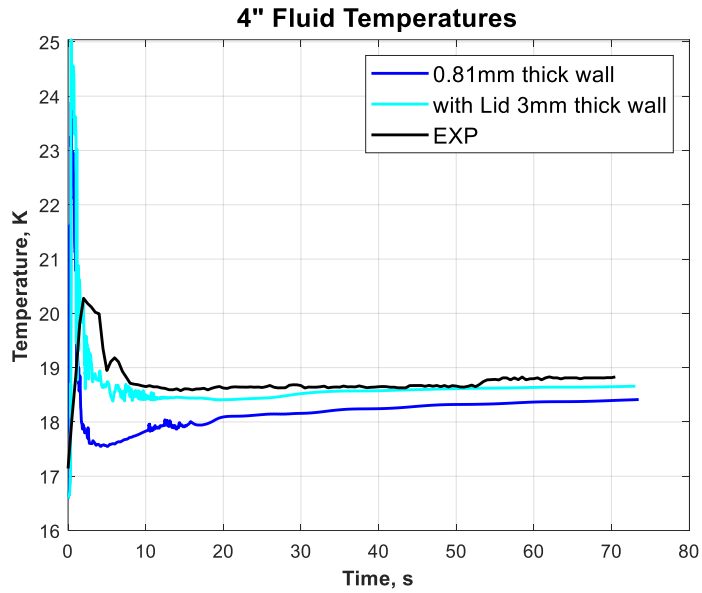
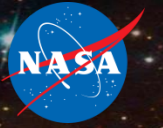




# Effect of Geometric Configuration (4 of 4): Fluid Temperatures



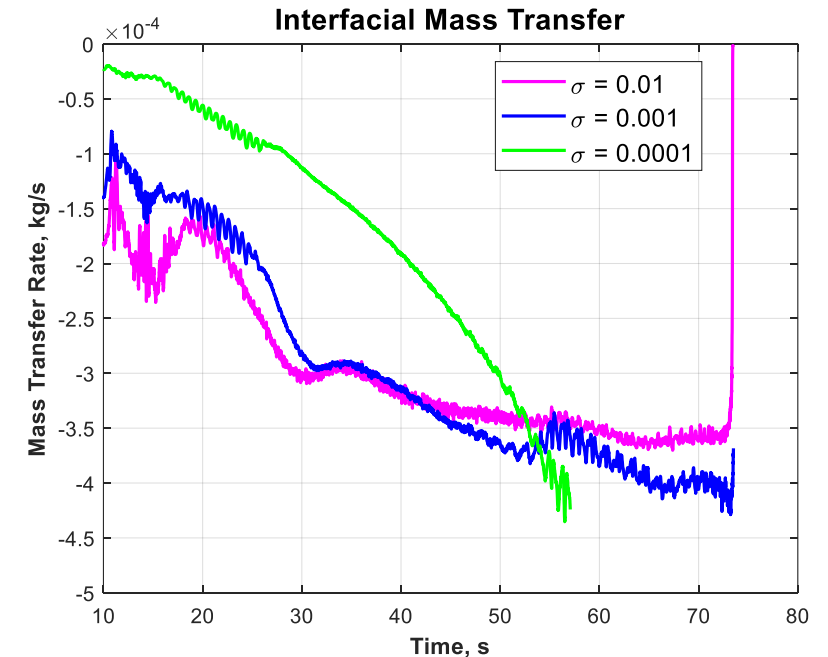
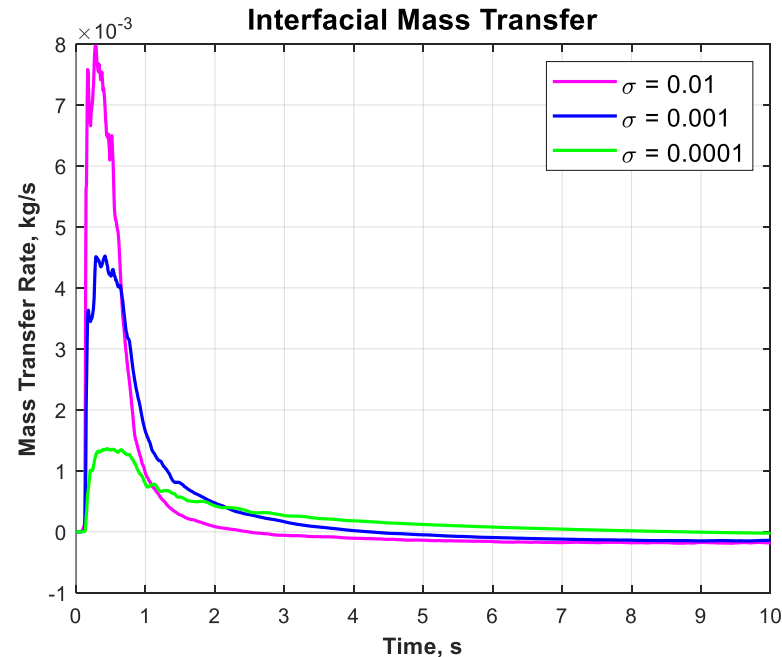
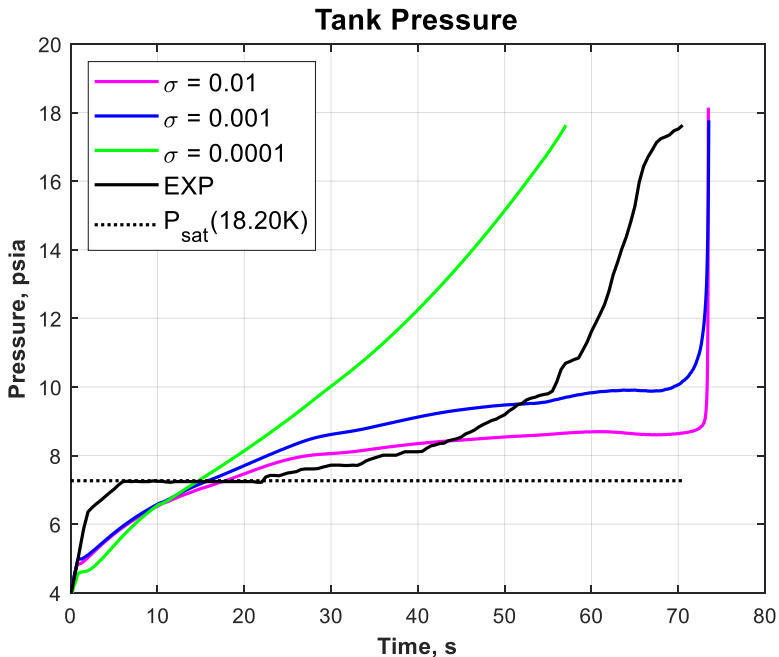
# Effect of Geometric Configuration (4 of 4): Fluid Temperatures



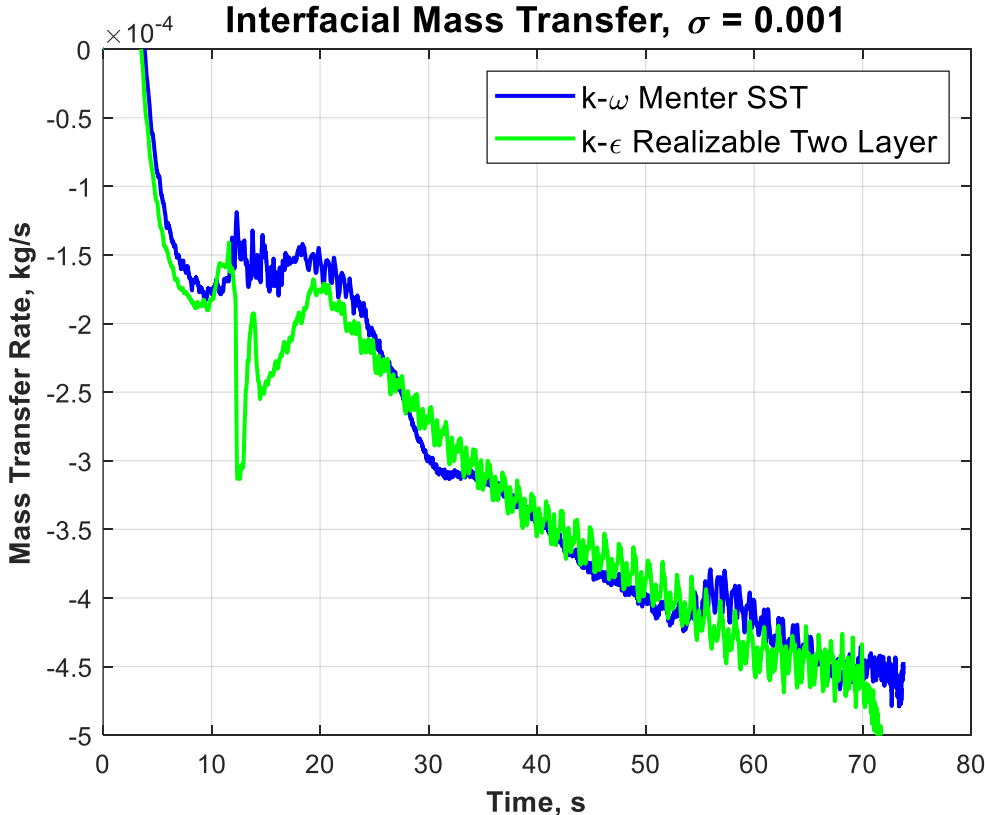
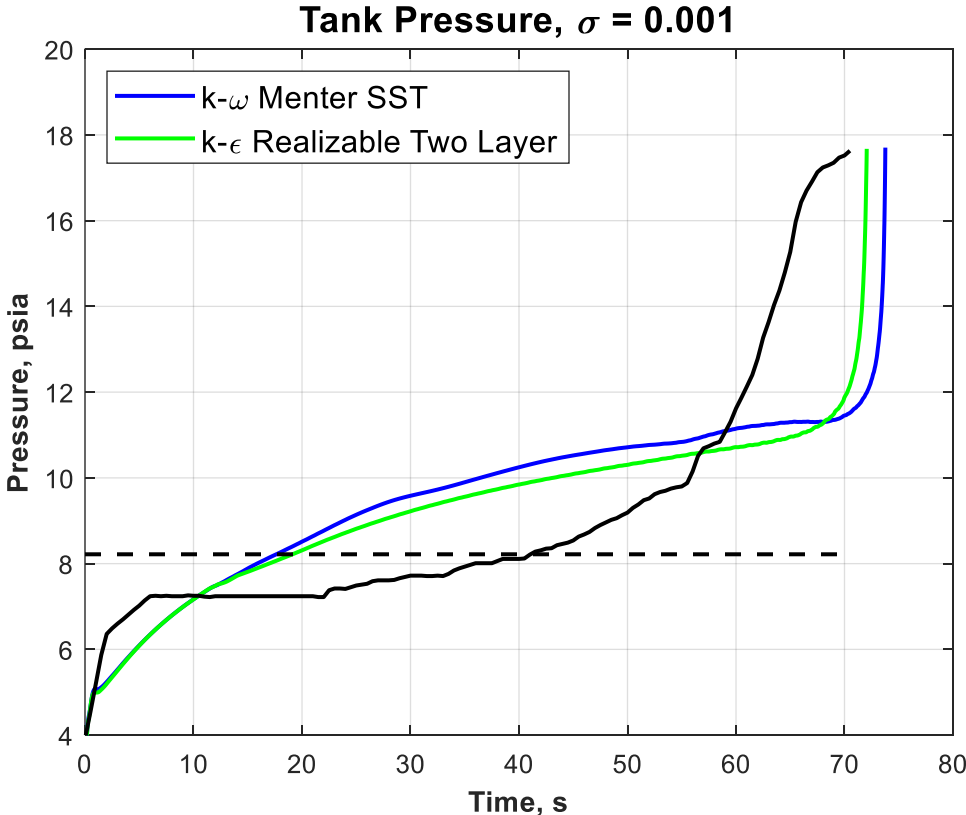
# Effect of Accommodation Coefficient



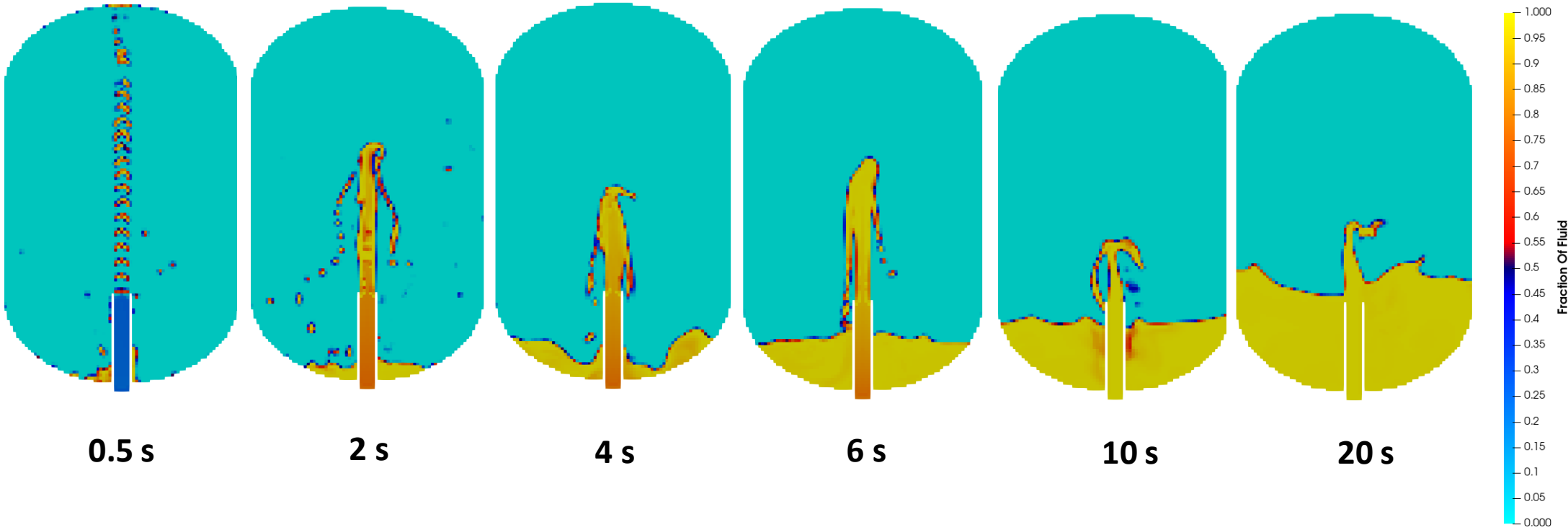
- Larger AC yields higher evaporation rates during beginning of fill and higher condensation rates during majority of fill
- Although  $\sigma = 0.01$  yields higher evaporation rates, mass transfer transitions to condensation earlier than the lower values
- Lower AC values yield higher condensation rates near end of tank fill because  $(P_{sat} - P_{abs})$  is large and negative



# Effect of Turbulence Model



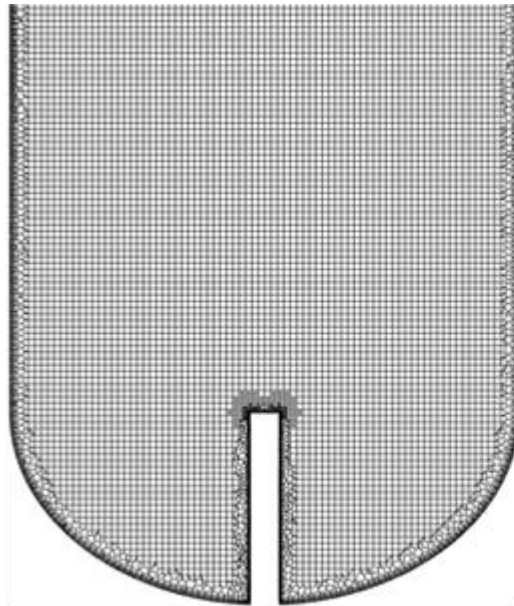
# Flow3D Phase Distribution



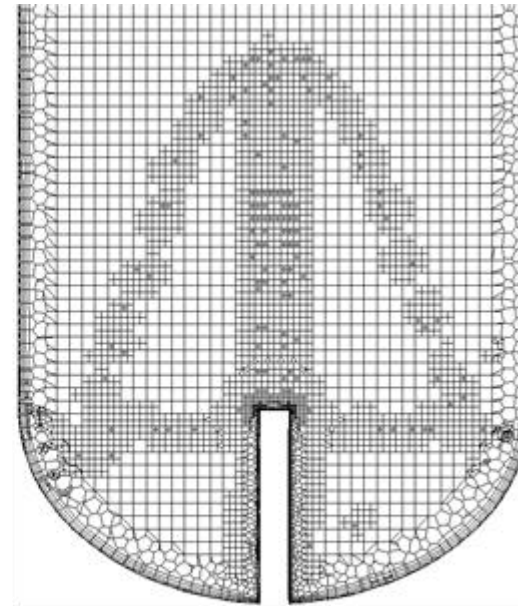
# Fluent AMR Speed-up



- Static mesh run-time = 497 hours
- Adaptive Mesh Refinement run-time = 280 hours
- ~40% decrease in run-time



No AMR (4mm-base, const)



AMR (8mm-base, adaptive)